NANOCHARACTERIZATION AND HEME-OXYGENASE 1 INDUCTION BY A NOVEL NANOFORMULATED BOTANICAL

by

Benny Habiyambere

Submitted in partial fulfilment of the requirements

for the degree of Master of Science

at

Dalhousie University

Halifax, Nova Scotia

December 2023

DEDICATION PAGE

I would like to dedicate this present thesis to my family: my parents, Claudine and Venuste and my siblings Destin, Victor and Marylise (in no order of favoritism obviously). I wouldn't be where I am with my academic journey if not for the constant support, love and belief you guys have for me.

TABLE OF CONTENTS

LIST OF TABLES

LIST OF FIGURES

ABSTRACT

Plants naturally synthesize nanoparticles to transport cellular materials that contain potential active pharmaceutical ingredients (APIs). Curcuminoids (e.g. curcumin) are the most abundant APIs in turmeric spice (from the *Curcuma Longa* plant), a traditional medicine with anti-oxidative/anti-inflammatory effects. Numerous chronic diseases largely feature oxidative stress and excess inflammation at the level of the macrophage. Curcumin is GRAS by the FDA but has poor stability, solubility and bioavailability. Nano-encapsulation of curcumin can improve its stability, solubility and bioavailability to elicit meaningful pharmacological effects. PVDL-005 (nanoparticles of curcumin) were spherical in shape, with a size and surface charge of 177 nm and -0.189 mV, respectively. PVDL-005 $[5\mu M]_{eq}$ induced 2-fold more heme-oxygenase-1 (HMOX1) than 5[μM] pure curcumin in THP-1 human macrophages. PVDL-005 was internalized more (i.e., vs curcumin) by macrophages and localized in the cytoplasm and nucleus. Our data suggests that administration of curcumin/PVDL-005 in the presence H_2O_2 does not confer cytoprotection *in vitro*.

LIST OF ABBREVIATIONS AND SYMBOLS USED

AAPH	2,2'-Azobis(2-amidinopropane) dihydrochloride
ADME	Absorption, metabolism, distribution, excretion
AP-1	Activator protein-1
API	Active pharmaceutical ingredient
ATCC	American type tissue culture collection
BBB	Blood Brain Barrier
BSA	Bovine serum albumin
CAT	Catalase
CD68	Cell differentiation 68
COX-2	Cyclooxygenase-2
DCFH-DA	2'-7'-Dichlorodihydrofluorescein diacetate
DLS	Dynamic light scattering
EMA	European Medicines Agency
FACs	Fluorescent assorted cell sorting
FBS	Fetal Bovine Serum
FDA	Food and Drug Administration
FL2	Flow channel 2
FRAP	Ferric reductive antioxidant potential
GCP	Good Clinical Practice
GMP	Good manufacturing practices
GRAS	Generally Regarded As Safe
GSH	Glutathione
H_2O_2	Hydrogen peroxide
HMOX1	Heme-oxygenase-1
HUVECs	Human umbilical vein endothelial cells
IL-1	Interleukin-1
IL-10	Interleukin-10
IL-12	Interleukin-12
IL-4	Interleukin-4
INF-γ	Interferon-gamma
INT	Iodonitrotetrazolium chloride
LDH	Lactate Dehydrogenase
LNP	Lipid-nanoparticle
LPS	Lipopolysaccharide
M1	Pro-inflammatory macrophages
M2	Anti-inflammatory macrophages
MI	Myocardial Infarction
MMPs	Matrix Metalloproteinases
MTT	3-(4,5-dimethylthiazol-2yl-)-2,5-diphenyl-2H-tetrazolium bromide
NAC	N-Acetyl-L-Cysteine
NF-κB	Nuclear factor kappa light chain enhancer of B cells
Nrf2	Nuclear factor erythroid 2-related factor 2
OD	Optical density
p-Nrf2	Phosphorylated nuclear factor erythroid 2-related factor 2

PBS	Phosphate buffer saline
PLGA	Poly(lactic-co-glycolic acid)
PMA	Phorbol 12-myristate 13-acetate
QAC	Quality assurance and control
ROS	Reactive Oxygen Species
RPMI-1640	Roswell Park Memorial Institute 1640
SnPP	Tin protoporphyrin IX
SOD	Superoxide dismutase
TAC	Total antioxidant capacity
TBST	Tris-buffered-saline-tween
TEER	Transendothelial electrical resistance/resistivity
TEM	Transmission electron microscopy
TGF- β1	Transforming growth factor beta-1
TNF- α	Tumor necrosis factor alpha
TPTZ	2,4,6-Tris(2-pyridyl)-2-triazine
TRPA1	Transient receptor potential cation channel A1

ACKNOWLEDGEMENTS

I would like to acknowledge my supervisor, Keith, who constantly strives to get the best out of me as a graduate student by providing me with the necessary tools, support and opportunities. To my laboratory colleagues (past and present), Kyle, Minji, Ashley, Tori and Vikki for always being supportive and assisting me the best way they could. To staff members and laboratory technicians at DMNB and UNBSJ for making resources available that were instrumental in this process.

Chapter 1 Introduction

1.1 The role of macrophages in pathophysiology

In the event of injury, tissues classically undergo four phases of: haemostasis, inflammation and granulation, tissue proliferation and remodeling[1]. Acute wounds progress through the healing phase with minor complications, but chronic wounds are characterized by a delay in the inflammatory phase and may never heal even with therapeutic intervention[2]. Haemostasis is the first stage that involves the recruitment of platelets to the site of injury to limit blood loss[1]. Resident macrophages or recruited monocytes (i.e., which eventually differentiate into macrophages) as well as other immune cells localize at the site of injury. This triggers the inflammatory phase as macrophages produce cytokines and reactive oxygen species (ROS) in response to their heighted metabolic activity at the site of injury. Macrophages will elicit recruitment of tissue resident cells or fibroblasts (i.e., via release of chemokines) and endothelial cells that promote angiogenesis. The tissue remodeling phase involves the restoration or modification of the tissue to stabilize its structure. Fibroblasts will produce extracellular matrix forming scar tissue if localized tissue regeneration is insufficient[1]. This stage is heavily mediated by the activity of matrix metalloproteinases (MMPs). MMPs are a family of proteinases that play an important role in the proteolytical degradation of the extracellular matrix[3]. Macrophages produce their own MMPs that can degrade the scarred tissue and allow for further tissue remodeling[1]. These inflammatory cells also release paracrine factors that enable wound healing and tissue restoration[1]. Macrophages and their function are not homogenous nor dichotomous, but rather heterogenous on a spectrum of polarization[1]. Macrophage polarization refers to the activation of macrophages by microorganisms, cytokines, inflammatory response or other physicochemical factors that cause these cells to differentiate into different phenotypes depending on the state and changes in their microenvironment[4]. Macrophages are generally classified as pro-inflammatory

(M1), or inflammation resolving/pro-regenerative (M2). M1 macrophages are associated with early injury events, which are present shortly after a wound is formed. M2 macrophages are associated with anti-inflammatory and pro-regenerative events. For example, with myocardial infarction (MI), impaired or delayed wound healing can cause the injured tissue to remain in a constant state of inflammation (e.g., via heightened M1 activity) risking ventricular rupture or scar thickening and myofibrosis formation to promote stability (contributed in part by M2 activity)[1]. There is interest in identifying drugs and mechanisms of action that promote the anti-inflammatory phase or minimize inflammatory phase as a therapeutic strategy for several diseases (i.e., polarizing macrophages away from an inflammatory M1 and towards an anti-inflammatory M2 phenotype by pharmacological intervention)[1].

MI is the leading cause of heart failure related morbidity and mortality[5]. This pathology features ischemia, where blood supply within the heart is arrested transiently or permanently. The surviving cardiac tissue have elevated workloads to pump blood to the rest of the body. Monocytes and macrophages are activated during an MI as they provide immune surveillance (albeit this is a sterile inflammation), regulate necrotic tissue clearance, support cardiac function and direct wound healing[5]. Sterile inflammation occurs in the absence of microorganisms (i.e., induced immune response) caused by the release of intracellular contents by inflammatory cells (i.e., macrophages, necrotic cells)[6]. Macrophages have a role in localized haemostasis, inflammatory phases, proliferative and tissue remodeling of the injured heart tissue. In a healthy heart, resident monocytes and macrophages are also critical to the normal function and homeostasis of the heart[5]. After MI, splenic and bone marrow monocytes (i.e., mononuclear cells differentiate into macrophages at the site of injury due to cytokines and chemokines released by resident macrophages) and macrophages are recruited to the site of injury, which promote further inflammation[5]. M2 macrophages release TGF- β1, which is important for fibroblast to myofibroblast transformation for tissue regeneration[7]. Desmouliere *et al*. showed *in vitro* experiments that neutralization of TGF- β1 using antibodies results in a decrease

in α-smooth muscle actin, a key mediator in myofibroblast differentiation during wound healing[7]. An *in vivo* model of acute MI shows that inflammation in the infarct drives monocyte migration from the spleen and removal of the spleen led to worsening of the injury and accelerated heart failure[8]. They also noted that the levels of inflammatory mediators, such as TNF-α were elevated. All of these factors led to delayed wound healing, including secondary injuries of the heart[8]. As such, comorbid conditions that impact one system can alter the pathophysiological regulation of macrophages systemically. Modified sterile inflammation by disease can potentially worsen outcomes partly due to variations in macrophage polarization or cellular constituents and their associated regulatory paracrine factors available to participate in wound healing.

Diabetes is a major comorbid metabolic disease to many other inflammatory diseases or ischemic tissue damage and is characterized by an increase in blood glucose levels due to insulin resistance and insulin deficiency[9]. These patients will likely develop some form of skin wounds or foot ulceration. Nearly 15% of all patients with Type 2 diabetes will develop diabetic foot ulcers, one of the most severe types of diabetic wounds often exacerbated by nervous tissue damage that alters pain sensing. This can present two major adverse outcomes: lower limb amputation or death. There is evidence suggesting that hyperglycemia can negatively impact monocyte recruitment to sites of injury, though which category and when remains to be fully defined in patients[9]. Diabetic mice showed increased resident monocytes before the skin wound and this was maintained following the injury compared to healthy mice[10]. These macrophages showed a propensity to polarize to the M1 phenotype, and this exacerbated the inflammatory events of diabetes further[10]. Mirza *et al.* showed that when macrophages were absent in injured mice (i.e., skin injury), they experienced delayed endothelial cell migration, decreased cell proliferation, and reduced collagen formation[11]. This emphasizes that there are critical roles of various macrophages to wound healing and recovery. Macrophages generally respond to damage associated molecular patterns, clearing debris from necrotic cells, and

signaling to other cells temporally, where it is appropriate to regenerate or remodel the tissue.

Pain is described as an unpleasant sensory and emotional experience associated with, or resembling that associated with, actual or potential tissue damage[12]. It is caused by the activation of primary nociceptors in response to noxious or potentially damaging stimuli, where inflammation is the major cause of disease[13]. Pro-inflammatory M1 macrophages elicit pain by the release of inflammatory cytokines that activate nociceptors[14]. ROS generated by macrophages can also interact with TRPA1 nociceptors , where the stimulation of this channel could lead to chronic development of neuropathic pain and diabetes[14,15]. Macrophages can also play an important role in pain resolution as they release IL-10, pro-resolving mediator, that induces expression of cytoprotective enzymes like heme-oxygenase-1 (HMOX1), as well as molecules like neuroprotectin-D1 and β-endorphin to interact to nociceptors and promote analgesic effects[14].

After tissue injury, a common damage associated molecular pattern—due to hemostasis, rupture of localized cells or the release of mitochondria into the extracellular space—is a localized elevation in heme and hemeproteins that macrophages phagocytose[16]. Macrophages are a major source of heme metabolism and HMOX1 expression[17]. HMOX1 protein is an inducible enzyme that produces carbon monoxide and bilirubin as byproducts of heme catabolism. Carbon monoxide and bilirubin (i.e., potent antioxidant) can exert anti-inflammatory and anti-oxidative effects to help with wound healing. Macrophages produce cytokines and ROS in response to heightened metabolism during wound healing, risking damage to themselves or proximal cells. This requires them to compensate with intrinsic antioxidant effects (e.g., by autocrine or paracrine mediate HMOX1 protein expression)[17]. An increase in HMOX1 protein expression has been shown to promote polarization of macrophages to an M2 phenotype[18]. In diabetic nephropathy, inflammatory M1 and anti-inflammatory M2 macrophages are both present in the disease microenvironment.

Upregulation of HMOX1 is cytoprotective and promotes an anti-inflammatory phenotype to release IL-10 to lower inflammation and promote wound healing in diabetes[19].

THP-1 cells are a commonly used immortalized human cell line to model monocytes and macrophages *in vitro*[20]. THP-1 non-adherent monocytes can differentiate to adherent macrophages in the presence of phorbol 12-myristate 13-acetate (PMA). These cells are also responsive to cytokines that can elicit polarization into M1/M2-like cells[20]. Fetal Bovine Serum (FBS) is formed by removing fibrin from fetal bovine plasma, and it contains hormones, fats, and many potent small molecules or growth factors[21]. A majority of *a priori* information using THP-1 cell culture rely on 10% FBS-supplemented media. Caution should therefore be considered when working with FBS. It is useful to expand THP-1 monocyte cells for study, but could also interfere with polarization, or interpretations of drug/stimulus responses[22]. As such, methods for quality assurance and controls are best suited to low serum or serum-free or chemically defined media conditions and method development is important to model monocyte/macrophage pathophysiology and drug responses[22,23].

1.2 Turmeric and curcumin as a traditional medicine

Turmeric (from the *Curcuma Longa* plant) has a long history as a traditional medicine for its claimed anti-inflammatory and anti-oxidative effects. Turmeric is a complex plant with notable potential active pharmaceutical ingredients (APIs), mostly composed of curcuminoids such as curcumin, derivatives of curcumin include desmethoxycurcumin and bisdemethoxycurcumin as well as other compounds like flavonoids and terpenes[24]. Turmeric's medicinal use was heavily prescribed in Asia. It was widely used in traditional Chinese medicine for a range of skin disorders and gastrointestinal disorders (i.e., to improve digestion)[25]. In Islamic medicine, the turmeric spice was recommended for obstructive jaundice and epilepsy, while the wood from turmeric was used of alleviate tooth pain. Traditionally, Indian subcontinent cultures ascribed anti-fever, wound healing and anti-nausea effects to turmeric[25]. Curcumin (diferuloyl

methane) is a yellow polyphenolic compound and the most abundant potential API in turmeric. An API refers to the compound in the drug formulation expected to produce the desired pharmacological effect[26]. Many of turmeric's medicinal properties can be attributed to curcumin, making it the most plausible API for turmeric[27]. Curcumin's therapeutic potential has been observed in patients with cardiovascular, diabetes, and arthritis[27]. Numerous *in vitro* studies have explored the potential benefits of curcumin, yet there are many absorbance and fluorescence based assays that can be mis-interpreted and were not properly controlled or calibrated to ensure rigour and reproducibility. Despite evidence in human and veterinary sciences utilizing this API clinically and *in vivo*, curcumin absorption, distribution, metabolism and excretion (ADME) make it a poor candidate for classical pharmaceutical development due to limited bioavailability[26 for detailed review]. In summation, clinical and pre-clinical studies have been performed using oral formulations of curcumin and it was determined that the amount of curcumin detected in blood serum/plasma was minimal/negligible. For example, oral bioavailability of 12 g/day curcumin in rats is less than 1%, partly this may be due to its hydrophobicity or transformation that limits absorption. Further, after absorption curcumin can be metabolized by Phase I enzymes (e.g., alcohol dehydrogenase) and Phase II metabolism through glucuronide conjugation. While a majority of orally administered curcumin to rats is excreted in feces and some is also detected in urine in an unmodified form, indicate of renal excretion without metabolism. Some metabolites of curcumin have been detected in rat and human plasma. The overall ADME profile of curcumin is therefore poor and thus new curcumin formulation methods should be investigated to improve curcumin's medicinal potential.

1.3 Therapeutic potential of nanoparticles

Doxil, a pegylated liposomal doxorubicin, was the first ever approved drug-loaded nanoparticle formulation approved by the FDA. It was an improved formulation of doxorubicin and it showed to have a higher safety profile compared to other drugs indicated for breast cancer[29]. The field of nanomedicine

emerged from researcher motivations "*to provide a long-circulating drug reservoir from which the drug can be released into vascular compartment in a continuous and controlled manner.*" [30] Nanoparticles can be as: polymeric, inorganic, or lipid-based. Lipid-based nanoparticles (i.e., liposome, lipid nanoparticles or emulsions) are the most common class of FDA-approved nanomedicines as they offer many advantages that include formulation simplicity, biocompatibility, and high bioavailability[31]. Liposomes are a subset of lipid-based nanoparticles that are typically composed of phospholipids, which can form unilamellar and multilamellar vesicles[31]. Liposomal nanoparticles can be used to encapsulate hydrophobic and lipophilic compounds and their *in vitro* and *in vivo* stability are conditional to nanoparticle size, surface charge, lipid composition and surface modifications (e.g., ligands). Another subset of lipid-based nanoparticles are lipid nanoparticles (LNPs), which are generally used for the delivery of nucleic acids. LNPs are characterized by four major components: ionizable lipids that form a complex with negatively charged genetic material to assist in endosomal escape, phospholipids and cholesterol for stability and structure and membrane fusion, PEGylated lipids (i.e., having polyethylene glycol or PEG polymer chains attached to the nanoparticle) to improve stability and circulation. LNPs differ from liposomes in that they form micellular sub-structures within the nanoparticle core, which can be modified during nanoparticle synthesis[31]. The use of synthetic excipients can cause undesirable and detrimental effects relating to toxicity, activation of the host immune response and unwanted biodegradability[32]. Plant extracelluar vesicles (including: exosomes, microvesicles, apoptosomes and other endogenous nanovesicles) can be similar to liposomes and present in turmeric where they are used to transport cargo (i.e., containing the API) between plant cells. Nanovesicles found in turmeric can be isolated for medicinal potential[33]. Harnessing the intrinsic properties of a biological nanoparticle (i.e., turmeric) formation in an extraction/extrusion of nanoparticles for therapeutic and pharmacological use is highly promising. The isolation of endogenous nanovesicles from whole plant mass may avoid undesirable effects (i.e.,

toxicity/poor safety, lowered tolerogenicity) and improve reliable drug delivery as an alternative to use of synthetic nanoparticles[32].

Two clinical trials evaluating nanoparticle formulations of curcumin for acute pancreatitis (NCT04989166) or colon cancer (NCT01294072) seek to determine whether nanoformulations are sufficient to elicit efficacy and overcome ADME limitations. Both these studies were recently completed but results from the trials are yet to be posted. For the trial involving acute pancreatitis, clinicians and researchers involved in the trial are investigating if nanocurcumin supplementation can improve clinical outcomes such as promoting analgesic effects (i.e., inflammation, lowering of abdominal pain intensity) in mild and moderate acute pancreatitis (NCT04989166). They are also interested in whether the intervention would impact hospital stay and/or readmission (NCT04989166). In the colon cancer trial, they are interested in exploring the purported anti-cancer effects for curcumin's ability to inhibit colon carcinogenesis (NCT01294072). The primary outcome is to assess safety and tolerability of curcumin and curcumin encapsulated plant exosomes (i.e., from fruits and vegetables) in normal and cancerous tissues, the effect of curcumin and nanocurcumin on immune and metabolic response of normal and cancerous colon tissue (NCT01294072). Several studies show that a nano-delivery based approach improved the bioavailability and therapeutic efficacy of curcumin *in vitro* and *in vivo*. For example, curcumin encapsulated solid-lipid nanoparticles have been shown to be a potent immunoregulator able to modify pre-clinical outcomes to LPS-induced sepsis by modulating the inflammatory pathways[34]. Curcumin-loaded on polyethene gel-graphene quantum dots has a reported benefit in a rodent model of MI after intraperitoneal administration that was superior to curcumin alone at the same relative concentration. This led to a reduction in infarct size and fibrosis[35]. Interestingly, curcumin has also been shown exert anti-oncogenic effects (i.e., by exerting pro-oxidant effects). For example, primary leukemia cells treated with concentrations of curcumin >10[μM] caused decrease in glutathione levels[36]. How this API elicits cytoprotection and chemotherapy benefits remains to fully reconciled.

1.4 Rationale

Curcumin is considered Generally Regarded as Safe (GRAS) by the FDA (GRN 822) but its poor bioavailability, instability, and rapid excretion *in vivo* makes it challenging to develop it as an API with clinical benefit. Development of various delivery systems (nanoparticles, microparticles, hydrogels or biomaterials) could improve curcumin's drug profile[37].

Curcumin exerts a direct antioxidative action by donating a proton to reactive oxygen species (ROS) to stabilize and lower their reactive potential (Fig-1). Curcumin's indirect antioxidative effect can be mediated through induction of the HMOX1, which leads to the synthesis of bilirubin, a potent antioxidant that targets ROS and promotes cell survival (Fig-1) [38]. Gupta *et al.* showed the simultaneous administration of H_2O_2 with curcumin encapsulated poly(beta-amino ester) nanoparticles promoted cytoprotective benefit from H_2O_2-induced endothelial cell death[39]. A 6hr pre-treatment of curcumin and its derivatives were shown to be cytoprotective in H_2O_2-induced death of endothelial cells via induction of HMOX1[40].

A.

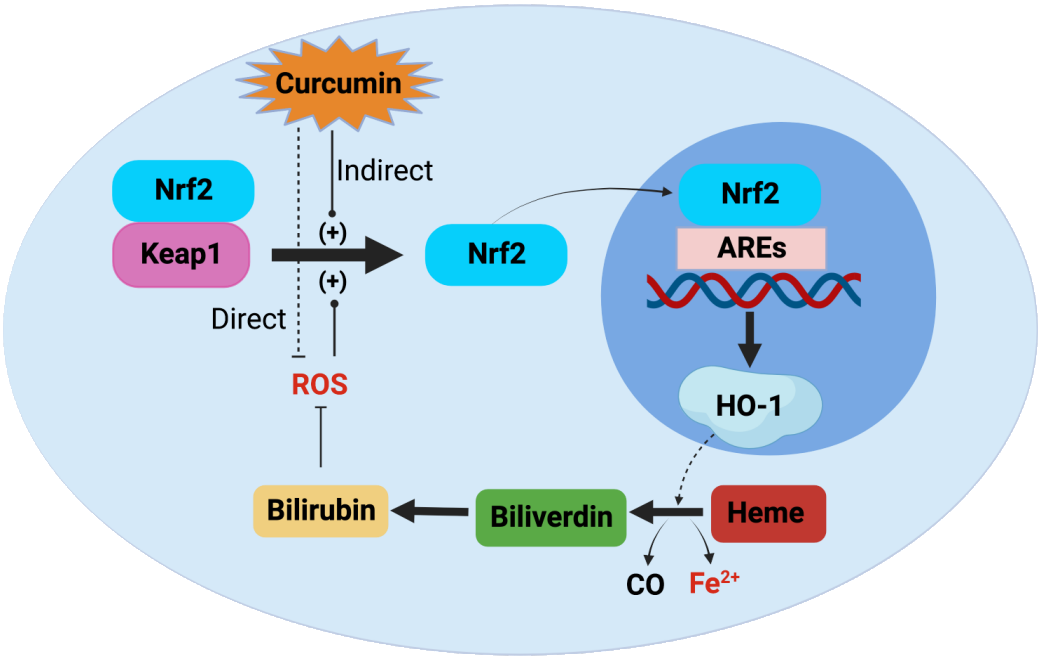

Figure 1: ***Direct and indirect intracellular signal transduction pathway of curcumin.***

AREs= Antioxidant Response Elements, HO-1= Heme-oxygenase-1 or HMOX1 protein, ROS= Reactive oxygen species.

Macrophages are a likely target of liposomal drug delivery due to their high endocytic and phagocytic activity, which make them both a risk of adverse effects to nanoparticle uptake but also a potential target to modify inflammation[30]. For example, a liposomal formulation of amphotericin B (i.e., ambisome) was delivered to fight parasites within macrophages[30]. The nano-encapsulation of an API into a nanoparticle can improve drug bioavailability, stability, and solubility and can be intentionally designed for uptake by macrophage phagocytosis. Macrophages that might otherwise cause damage to themselves or surrounding tissues after injury could therefore benefit from uptake of nano-encapsulated curcumin, as a means of reduced ROS or modifying the cytokine profile to be less pro-inflammatory or more anti-inflammatory.

1.5 Hypothesis and objectives

Hypothesis: Extracted/extruded turmeric root nanoparticles will elicit greater direct antioxidative and/or indirect cytoprotective effects via curcumin-mediated HMOX1 induction in human macrophages compared to a molar equivalent amount of curcumin.

Objectives: 1) Establish quality assurance and control (QAC) methods for the biophysical characterization of nanoparticle properties. 2) Establish QAC methods for a reference-based determination of the molar equivalents of nanoparticles to curcumin API and establish a reference-based analysis of direct total antioxidant capacity, 3) Establish the equivalency of a select nanoparticle using THP-1 human macrophages for induction of HMOX1 at molar equivalency to reference curcumin. 4) Determine uptake, internalization and localization of a select nanoparticle in macrophages *in vitro*. 5) Determine the safety profile of a select nanoparticles in macrophages *in vitro*. 6) Determine the cytoprotective efficacy of a select nanoparticle to a stress challenge of high-dose H_2O_2 either by prophylaxis or interventional (simultaneous) treatment with a select nanoparticle.

Chapter 2: Materials and Methods

2.1 Turmeric nanoparticle preparation

Botanical extracts were extruded and nanoformulated by proprietary processing by Pividl Bioscience Inc. to establish a routine QAC (i.e., analytical, biophysical), biochemical (i.e., antioxidant capacity) and *in vitro* equivalency (i,e., to a reference agent), safety, and efficacy experiments. The following preparations of PVDL nanoparticles, PVDL-000/-001/-004/-005 (nanoformulated from turmeric root extracts) and PVDL-002/-003 (nanoformulated from the extraction of turmeric root combined with 3 other botanicals) were used in this research. The empty-nano vehicle was a PVDL nanoparticle formulated from yeast extracts. All PVDL nanoparticles (including the empty-nano) were suspended in liquid vehicle excipients involving the combination of saline, ethanol, or bovine serum. Nanoformulations of PVDL nanoparticles from the turmeric extracts were dialyzed using Slide-A-Lyzer® G2 dialysis cassettes (VWR, Cat# CAPI87718) (to remove constituents of the liquid vehicle excipients with a molecular weight >2K), then filtered with 0.45µm sterile filters. Alternatively, PVDL nanoformulations that were not dialyzed were prepared in biosafety cabinets (Labconco^{TM}) to ensure nanoparticle sterility for *in vitro* experiments.

2.2 Dynamic Light Scattering (DLS)

The size and zeta potential of PVDL-005 was determined using a Zetasizer Nano ZSP (Malvern). For size analysis, a 10X dilution of PVDL-005/Empty-nano was performed in ddH_2O; 100µL and 800µL of PVDL-005/Empty-nano was added to a ZEN0040 cuvette (for size, Malvern #ZEN0040) and DTSS1070 (for zeta potential, Malvern #DTSS1070), respectively. Settings were selected as: protein for the measured material, water as the dispersant and the temperature was set at 25^{o}C. Three independent measurements of 12

readings each was performed for size and zeta potential analysis, with a 30s equilibration time between measurements.

2.3 UV-spectroscopy

Curcumin (Sigma-Aldrich, Cat#C1386) 37.5 mg was dissolved in 15mL of 98% ethanol to prepare a 2.5 [mg/mL] curcumin stock. The absolute curcumin concentration was 1.625 [mg/mL] or 4.41[mM] when adjusted for purity (>= 65% purity). Curcumin-ethanol standards (Stnd) of the following concentrations were prepared: 1, 2.5, 5, 10, 25, 50, 75, 100, 125 and 150[µM] in 98% ethanol. PVDL-005 curcumin equivalence (PVDL-005 curcumin $[\mu M]_{eq}$) was determined from the curcumin optical density (OD) or absorbance from the standard curve. The same standard curve was used to define the curcumin equivalence of all PVDL nanoparticles. Curcumin standards and stock were stored at 4^{o}C and used within 4 months. PVDL-005 stock was stored at 4^{o}C. Sample absorbance reading was blank-corrected, and all readings were performed using a Synergy H4 plate reader (Biotek) at λ_{430nm}.

2.4 Transmission electron microscopy (TEM)

PVDL-005 was directly deposited as 5 or 10 µl onto 200 mesh formvar/carbon grids and allowed to incubate at room temperature for 10 minutes before removing the excess liquid by wicking with filter paper. The grid was then sequentially washed twice for two minutes by floating sample-side down on two separate 100 µl of ddH_2O (0.22 µm mesh filtered) droplets on parafilm. Contrast staining was done by floating sample-side down on a 0.22 µm mesh filtered 1% uranyl acetate (Fisher Scientific Company) droplet for 1 minute. Grids were imaged with a STEM3+ detector on a Scios 2 DualBeam (Thermo Scientific) at 80,000 x magnification and 30 kV accelerating voltage. Preparation, imaging, and processing were conducted at the Microscopy and Microanalysis facility at the University of New Brunswick, Fredericton campus (Biology Department).

2.5 Antioxidant capacity

The total antioxidant capacity was determined according to the recommended procedures of the manufacturer of the Ferric Reduction Antioxidant Potential (FRAP) assay kit (ThermoFisher, Cat # EIAFECL2). Ferrous chloride [10mM] was diluted in 1X acetate buffer to prepare Fe^{2+} standards of 0, 31.25, 62.5, 125, 250, 500 and 1000[µM] by serial dilution. All samples (i.e., Curcumin, PVDL nanoparticles, ascorbic acid, NAC and gallic acid) were diluted in 1X assay buffer as: Curcumin samples of 50, 75, 100, 125 and 150 [µM]; PVDL-000/-001/-002/-003 of 108, 150, 56 and 57 $[\mu M]_{eq}$ and PVDL-005 of 80, 90, 100, 110, 120 and 130 $[\mu M]_{eq}$. An ascorbic acid positive control was diluted to 250[µM]. Fresh stock of N-Acetyl-L-Cysteine (NAC, Amresco Cat#0108-25G) was diluted in 1X PBS to 3[mM] and gallic acid in ddH_2O to 10[mM]. Then, NAC and gallic acid positive controls were prepared by diluting respective stocks in 1X assay buffer to 62.5, 125, 250, 500 and 1000[µM]. All Fe^{2+} standards and samples were vortexed and 20µL was added to appropriate wells (half-area 96-well plate supplied by kit). 75µL of the FRAP colour solution into each well and the plate was left to incubate for 30 minutes. A fresh Fe^{2+} standard curve was prepared for each assay, as recommended by vendor for QAC. The absorbance was read at 560nm using a Synergy H4 Hybrid Reader (Biotek).

2.6 THP-1 cell culture

THP-1 human monocytes were expanded from frozen stocks purchased from the American Type Tissue Culture Collection (ATCC) using plating media containing Roswell Park Memorial Institute-1640 (RPMI-1640; ThermoFisher Scientific CAT#A1049101) supplemented with 10% FBS (ThermoFisher Scientific CAT#12483020). Cells were passaged at least twice following recovery from cryogenic storage and did not exceed 20 passages. Cells were cultured at 37°C in a 95% air, 5% CO_2 humidified atmosphere and the media was replaced every 3-4 days on maintenance cultures.

2.7 THP-1 phorbol 12-myristate 13-acetate (PMA) differentiation

THP-1 proliferative monocytes were differentiated into adherent macrophages by diluting 10nM PMA (VWR, CAT#10187-494) directly in RPMI-1640-10% FBS media. After treatment with PMA, media was replenished with PMA-free RPMI-1640-10% FBS media and incubated for 24hrs for differentiation [41]. Treatments were then applied to differentiated macrophage cell cultures if following high FBS conditions. An additional incubation of 16hrs in RPMI-0.5% media is required before treatment if following low FBS conditions.

2.8 Western blot

THP-1 human monocytes were seeded at a density of $4x10^5$cells/35mm dish and differentiated in high FBS conditions (see method 2.7). Cells were then treated with 5[μM] curcumin, hemin or $[5\mu M]_{eq}$ PVDL-005 and harvested for comparative protein target analysis. Protein lysate samples and ladder were separated via SDS-polyacrylamide gel electrophoresis (Bio-Rad Cat# 5671095) and transferred onto nitrocellulose membrane (0.2μm, Bio-Rad# 1620112). Membranes were reversibly stained with MemCode (ThermoFisher Scientific Cat#24580) before immunoblotting. 5% milk was used to block for 45 min and incubated with (1:1000 or 1:10 000 in 1% skim milk in Tris-Buffered-Saline-Tween (TBST) with 4% sodium azide overnight. Membranes were washed in 1X TBS-T, followed by incubation with Goat Anti-Rabbit Horseradish Peroxidase-Conjugated Secondary Antibody in 5% milk (1:2000) for 2hr. The signal was detected by enhanced chemiluminescence (ThermoFisher Scientific #34076) and digital imaging. Western blot analysis was performed using Image Lab software and values were obtained by measuring the protein target relative to the total protein (MemCode).

2.9 Confocal microscopy

THP-1 cells were seeded at a density of $1x10^5$cells/well on EtOH sterilized and ddH_2O sterile rinsed coverslips placed in 6-well plates and differentiated in high FBS (see method 2.7) for treatment. Prior to fixation, the cells were washed

twice using 1X PBS. Cells were fixed using a solution of 3.7% formalin (VWR, Cat#16004-112) in 1X PBS for 10 minutes; washed for 5 minutes, 3 times each in 1X PBS and then permeabilized using 0.25% Triton X-100 for 10 minutes. Blocking was carried out using a solution of 1% BSA in 1X PBS with 0.1% Tween-20 for 20 minutes. Following blocking, cells were washed for 5 minutes, 3 times each in 1X PBS. Cells were then stained with a 1µL:1000µL dilution of Phalloidin 647 (in 1X PBS) (VWR, Cat#89427-130) for 30 minutes; then washed for 5 minutes, 3 times each in 1X PBS. A counterstain, Hoechest 33258 (ThermoFisher, Cat#62249) was used at a 0.5µL:10 000µL dilution for 1 minute. Cells were then washed for 5 minutes, 3 times each in 1X PBS. Coverslips with cells were carefully removed from the dishes and mounted on a microscope slide using PermaFluor mounting media (ThermoFisher, Cat#TA030FM) and sealed. Slides were allowed to dry overnight prior to imaging.

2.10 Flow cytometry

THP-1 monocytes were seeded at a density of $1.5x10^6$ cells/60 mm dish and differentiated in low FBS (see method 2.7). Cells were then treated with 2.5/5[µM] curcumin and PVDL-005 for 6hrs. Media was aspirated, and cells were washed twice with 1X PBS. Trypsin-EDTA (VWR, Cat#CA45000-658) was used to dissociate cells from plates. FACS buffer was prepared by weighing 0.2g of BSA (Cat#) in 200mL of 1X PBS and then sterile filtered using 0.22µm syringe filters. Cells were detached, and residual cells were collected by rinsing with FACS buffer and resuspending in 1ml of FACS buffer for immediate analysis. Otherwise, tubes were centrifuged at 4000 rcf for 4 min at room temperature. The supernatant was aspirated using a micropipette to minimize the disturbance of cell pellets. Fixing buffer was prepared by adding 10mL of 10% formalin to 40mL of 1X PBS. 1 mL of fixing buffer was added to all tubes and incubated at room temp for 30 min with intermittent mixing. The supernatant was aspirated using a micropipette. Cell pellets were washed twice with 1X PBS, followed by centrifugation and manual removal of supernatant by micropipetting. 200µL of FACs buffer was added to each tube. Cells were then stored at 4^oC for up to 5

days before performing FACs using the GalliosTM 10-color Flow Cytometer (Beckman Coulter). Curcumin's fluorescence was assessed in the FL2+ channel.

2.11 Cell viability

Cell viability was determined by the resazurin method. THP-1 human monocytes were seeded at $15x10^3$ cells/well in a 96-well plate with 100 µL media/well. FBS (Gibco) was freshly diluted in media to prepare treatments. H_2O_2 (Sigma-Aldrich Cat#323381) was freshly diluted in 10% or 0.5% FBS-supplemented media to a 100[mM] stock solution. Curcumin was prepared as a 1[mM] stock in sterile 98% ethanol. The turmeric-derived nanoparticles PVDL-004 (2 $[mM]_{eq}$ curcumin), and PVDL-005 (3.97$[mM]_{eq}$ curcumin) were suspended in a bovine serum + saline solution and ethanol + saline solution liquid vehicle excipient, respectively. NAC stock and treatment dose were freshly prepared following previously defined protocols [42–44]. First, 0.979g of NAC was diluted in FBS-free media to 600[mM] and then pH was adjusted to 7.4 using 1[M] sodium hydroxide, which further diluted the stock to 300[mM]. Then, 300[mM] NAC was sterilized using 0.22µm sterile filters and further diluted in FBS-free media to 15[mM] for treatment. The final 15[mM] NAC treatment was supplemented with sterile 0.5% FBS (the pH did not deviate from 7.4 after media supplementation with FBS). H_2O_2, curcumin and PVDL-004/-005 were further diluted in 10% and 0.5% FBS-supplemented media immediately before exposure to cells. 1.1[mM] and 2.1[mM] H_2O_2 negative controls were used at high and low FBS, respectively. Following cell treatments with the drug, 10 µL of PrestoBlue™ Cell Viability Reagent (Invitrogen) was added to each well and cells were incubated at 37ºC for 1 hr. Spectral fluorescence was measured using a Synergy H4 Hybrid Reader (Biotek) with excitation and emission wavelengths of 560 and 590 nm respectively. Cell viability was calculated by subtracting the fluorescence at 560/590nm media-only control or PVDL-005/Empty-nano/NAC-no cell control (i.e., to correct for curcumin's autofluorescence, 420nm-600nm or empty-nano or NAC interference) or curcumin/PVDL-005/Empty-nano/NAC + H_2O_2-no cell controls (i.e., to correct for any potential chemical interactions between

curcumin/PVDL-005/Empty-nano/NAC with H_2O_2) from the respective cell treatment groups and normalizing values to the mean viability of the untreated controls.

2.12 Statistical analysis

Graphical and statistical analyses were performed using GraphPad Prism (GraphPad Software Inc). Values are shown as mean ± standard deviation (SD) and/or percent difference (%) between groups. For comparison between three or more groups, a ONE-WAY ANOVA was used. ROUT method (Q=1%) was used to identify outliers.

Chapter 3: Results

3.1 Biophysical properties of PVDL-005

To determine the hydrodynamic size of nanoparticles, dynamic light scattering was used. To determine the colloidal stability, several dilutions of a nanoparticle preparation in ddH_2O showed an accurate and consistent measure of the nanoparticle average hydrodynamic size by intensity, when diluted between 5-15X for PVDL-005 (Fig-2 Aii). We elected to use intensity as a percent to demonstrate the high uniformity of the nanoformulation.

The PVDL-005 is a monodisperse sample, where individual nanoparticles were spherical (Fig-3 A), 177 nm in size (Fig-3 B) and exhibited a neutral charge on their surface by zeta potential (Fig-3 D). Zeta potential refers to the electrokinetic potential at the slipping plane of a colloidal nanoparticle. This plane is the interface that separates mobile particles and dispersant. Measuring zeta potential can inform nanoparticle colloidal stability[45]. The correlation coefficient (Fig-3 C) is a measure of how nanoparticles compare to one another over time. The curve is uniform, and the correlation coefficient is close to 1, indicating the nanoparticles are similar in their biophysical properties. The polydispersity index (PDI) (Fig-3 E) is a measure of nanoparticle size distribution, where a nanoparticle preparation can either be monodisperse (PDI, <0.7) or polydisperse (PDI, >0.7). Describing nanoparticle shape, size, and surface zeta potential is important as these biophysical parameters greatly impact nanoparticle stability and cellular internalization [46].

The nanoformulation of PVDL-005 (i.e., encapsulating curcumin) involved the extraction and isolation of turmeric nanovesicles from turmeric root biomass. As such, there is little opportunity to separate an empty nanoparticle, devoid of potential active pharmaceutical ingredients like curcumin, nor is it entirely possible to have just pure curcumin without some complex of excipients of various activities during the extraction and formulation processes. Generating a

nano-botanical negative nano-vehicle control as required by nano-pharmacology best practices therefore presents a challenge. The empty-nano-vehicle (empty-nano) used here was a botanical formulation generated from biomass with no known active pharmaceutical ingredients that Pividl Bioscience Inc. has developed for general drug or gene-loaded delivery or transfection. The empty-nano-vehicle approximated the biological effect of an empty nanoparticle for PVDL-005 and was handled in formulation preparations for QAC methods similarly after extraction. The empty-nano-vehicle and PVDL-005 had similar biophysical properties, supporting the rationale for using it as a control (Fig-4).

A.

i.

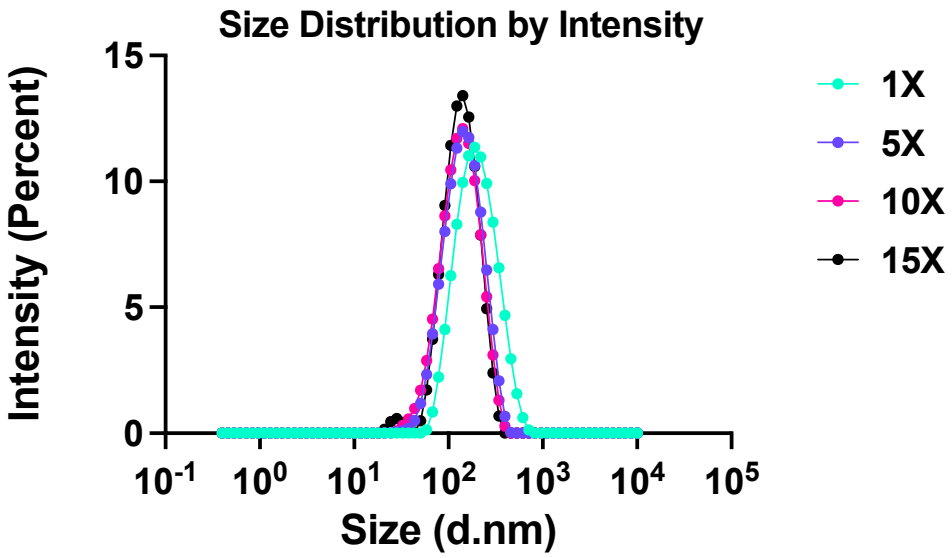

ii.

	1X	5X	10X	15X
Average Hydrodynamic size (d. nm)	354	192	177	183

Figure 2: ***Assessment of dilution conformity in nanoparticles hydrodynamic size of PVDL-005 by dynamic light scattering.***

Ai) Size distribution by logarithmic intensity for dilutions of PVDL-005 stock (1X,5X, 10X, 15X) in ddH_2O as a percent light intensity. Aii) Table of absolute average hydrodynamic size at all dilutions performed shows conformity at 5-15X dilutions in ddH_2O.

A.

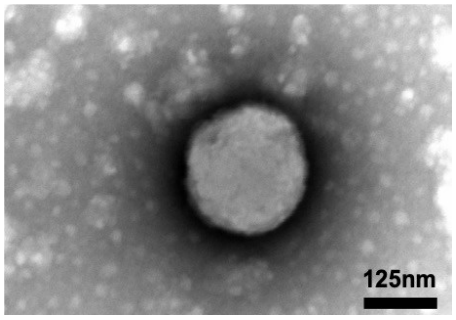

B.

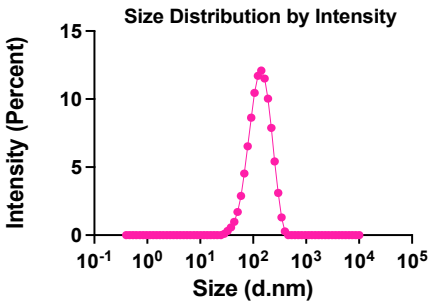

C.

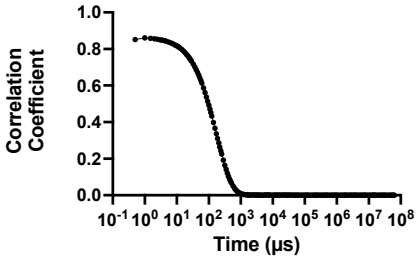

D.

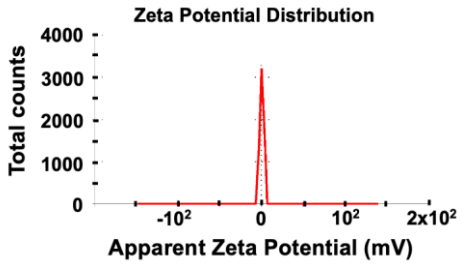

E.

Turmeric nanoparticle	Average hydrodynamic size (d.nm)	Polydispersity index (PDI)	Zeta Potential (mV)
PVDL-005	177	0.111	-0.189

Figure 3: ***Biophysical properties of PVDL-005 establish uniformity and conformity of nanoparticles with neutral surface charge.***

A) Transmission electron microscopy of nanoparticles shows spheroids of ~150nm in diameter. Dynamic light scattering was used to determine B) nanoparticle hydrodynamic size, C) nanoparticle uniformity by correlation coefficient and D) nanoparticle surface charge by zeta potential. E) Table outlining the polydispersity index calculated from, the absolute average hydrodynamic size (d. nm) and zeta potential (mV).

A.

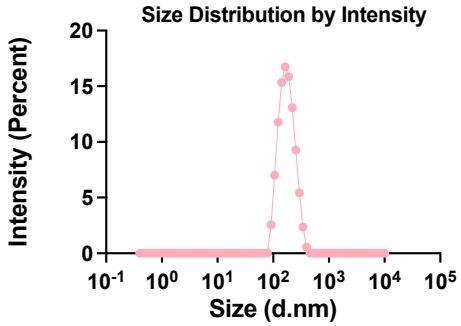

B.

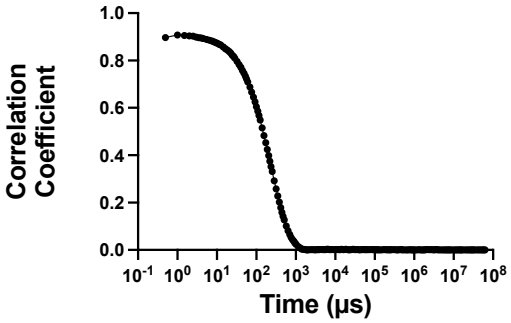

C.

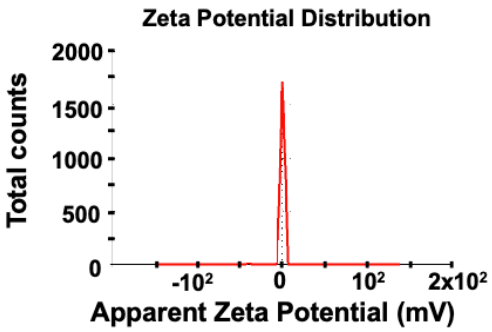

D.

Empty-Nano	
Average hydrodynamic size (d.nm)	165
Polydispersity index (PDI)	0.102
Zeta Potential (mV)	-0.251

Figure 4: ***The biophysical properties of the empty-nano reference are comparable to PVDL-005.***

The A) Size, B) Correlation coefficient and C) Zeta potential of empty-nano at a 10X dilution in ddH_2O. X-axis values are shown on a logarithmic scale. D) Table outlining the polydispersity index, the absolute average hydrodynamic size (d.nm) and zeta potential (mV).

3.2 Curcumin composition in PVDL-005

Curcumin and PVDL-005 derived from *Curcuma Longa* or turmeric root (i.e., containing curcuminoids) both absorb UV light at 430nm (Fig-5i and iii), which enable quantification of the presence of curcumin in the nanoformulation by spectroscopy. The concentration of curcumin standard is directly proportional to the OD or absorbance at 430nm (Fig-5ii), which is consistent with prior studies[47,48]. The unknown concentration of curcumin in PVDL-005 was thus determined from a curcumin standard curve at 430nm (Fig-5iv). Calculating the concentration of curcumin encapsulated in PVDL-005 were thus referenced in curcumin equivalence (or curcumin $[\mu M]_{eq}$) to enable testing and dosing of cells at molar equivalent curcumin concentrations.

A.

i.

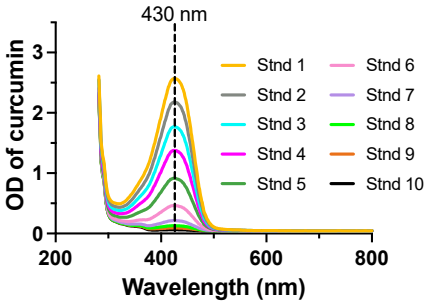

ii.

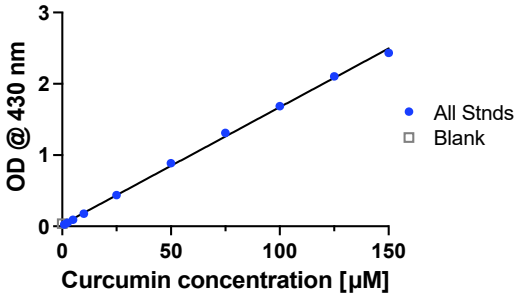

iii.

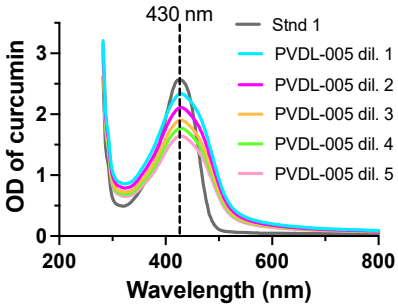

iv.

PVDL-005 dil.	OD of curcumin @430nm	PVDL-005 Curcumin $[\mu M]_{eq}$
1	2.3	135
2	2.0	121
3	1.8	110
4	1.7	101
5	1.6	94

Figure 5: ***Curcumin equivalence by absorbance.***

(i) Spectra of curcumin-ethanol standard (Stnd) and (ii) Curcumin-ethanol standard curve for all Stnds; Stnd 1=150[µM], Stnd 2=125[µM], Stnd 3=100[µM], Stnd 4=75[µM], Stnd 5=50[µM], Stnd 5=25[µM], Stnd 7=10[µM], Stnd 8=5[µM], Stnd 9=2.5[µM] and Stnd 10=1[µM]. (iii) Spectra for 5 different PVDL-005 dilutions (dil.) including a curcumin reference, Stdn 1. (iv) Calculated PVDL-005 curcumin equivalence, PVDL-005 Curcumin $[\mu M]_{eq}$, using the curcumin-ethanol standard curve.

3.3 Chemical antioxidant capacity of PVDL-005

Intracellularly, Fe3+ generates hydroxyl radicals by reacting with endogenous and/or exogenous H_2O_2 in an enzymatic-mediated reaction (Fenton reaction)[49]. The Ferric Reduction Antioxidant Potential (FRAP) assay measures the direct antioxidant capacity of known antioxidants (i.e., curcumin, N-acetylcysteine and gallic acid) by their ability to reduce Fe^{3+}-TPTZ to Fe^{2+}-TPTZ. The amount of Fe^{2+}-TPTZ produced at 560nm can be correlated to the antioxidant activity of a compound (Fig-6A).

Differences in the manufacturing of PVDL nanoformulations could impact the antioxidative potential of comparable amounts of curcumin. PVDL-000 and -001 were nanoformulated from the extraction of turmeric root biomass exclusively. Preparation of PVDL-002 and -003 involved the extraction of turmeric root (i.e., curcumin as its API) in concert with 3 other proprietary biomass sources of botanicals. The high antioxidant capacity of PVDL-002 and -003 is likely due to the added antioxidant effect of the combined botanicals along with curcumin (Fig-7C).

PVDL-005 curcumin $[\mu M]_{eq}$ is directly proportional to the amount of Fe^{2+} -TPTZ (Fig-8ii). PVDL-005 $[5\mu M]_{eq}$ produces minimal amounts of Fe^{2+} -TPTZ , which corresponds to low antioxidant capacity. NAC and gallic acid are potent antioxidants and were included as positive controls as reference antioxidants to curcumin and PVDL-005 in the assay. The antioxidant capacity of 125[μM] gallic acid is higher (+83%, $P<0.01$) than curcumin, whereas 125[μM] of NAC is lower (-274%) than curcumin. $125[\mu M]_{eq}$ PVDL-005 is higher than 125[μM] NAC (+150%, $P<0.01$) and 125[μM] of ascorbic acid (+19%, $P<0.01$). $125[\mu M]_{eq}$ PVDL-005 has a slightly lower but significant total antioxidant capacity compared to 125[μM] curcumin (-9%, $P<0.02$). 125[μM] curcumin was used as a reference since it had an equivalent concentration to prepared positive controls of 125 [μM] NAC and 125 [μM] gallic acid, allowing for simplicity in reporting the % antioxidant capacity. Taken together, we can express the total antioxidant

capacity (TAC) in reference to curcumin, gallic acid, NAC or ascorbic acid as a relative percent for ease of reporting or consistency (Fig-8iv).

A.

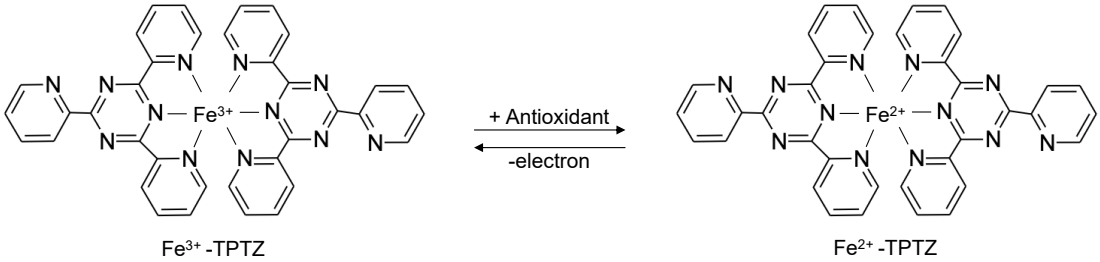

Figure 6: ***The reduction/oxidation equilibrium reaction measured by FRAP assay.***

A.

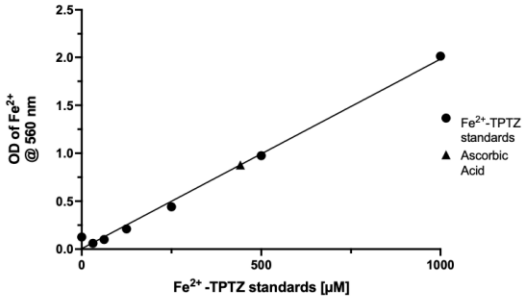

B.

Reference: 125µM Curcumin		
Sample	**Average OD of Fe^{2+}-TPTZ @560nm**	**Average Fe^{2+}-TPTZ [µM]**
Curcumin	0.52	259
PVDL Veh	0	0
PVDL-000	0.29	144
PVDL-001	0.65	327
PVDL-002	> 2.0	> 1000
PVDL-003	> 2.0	> 1000
Ascorbic acid	0.44	221

C.

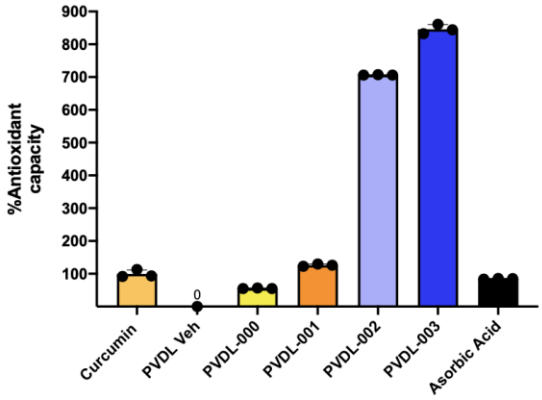

*Figure 7**: PVDL nanoparticles show potent chemical antioxidative potential by FRAP assay.***

A) Fe2+ -TPTZ [µM] standard curve, including a 250[µM] ascorbic acid positive control (supplied by FRAP assay kit). B) Determined average Fe2+ -TPTZ [µM] for each sample using the Fe2+ -TPTZ [µM] standard curve. Fe2+ -TPTZ [µM] for PVDL-002 and -003 fall outside the linear dynamic range of the Fe2+ -TPTZ [µM] standard curve, which is represented by “>2.0” and “>1000.” C) % Antioxidant capacity of PVDL Veh, PVDL-000, -001, -002, -003 and ascorbic acid relative to 125[µM] curcumin.

A.

i.

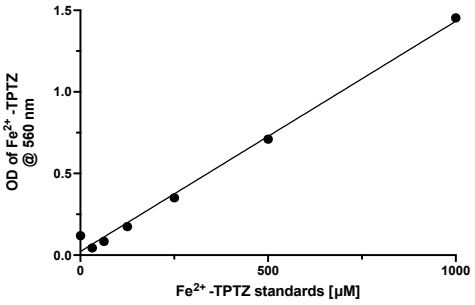

ii.

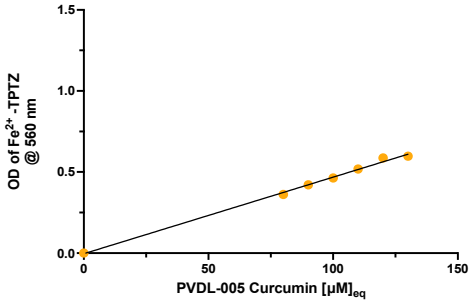

iii.

Reference: 125µM Curcumin		
Sample	**Average OD of Fe^{2+}-TPTZ @560nm**	**Average Fe^{2+}-TPTZ [µM]**
Curcumin	0.64	438
PVDL Veh	0	0
PVDL-005	0.59	400
NAC	0.25	160
Gallic Acid	1.2	802
Ascorbic Acid	0.49	336

iv.

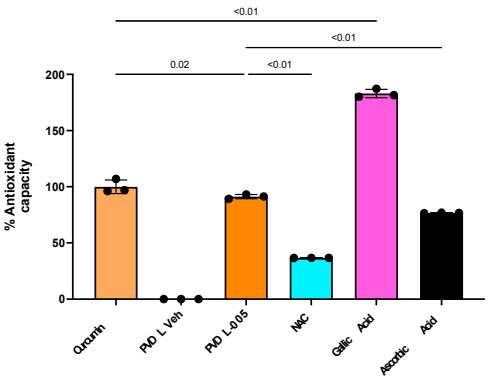

Figure 8: ***PVDL-005 shows direct antioxidant capacity by FRAP assay.***

(i) Fe^{2+} -TPTZ [µM] standard curve, (ii) OD of Fe^{2+}-TPTZ at 560nm relative to PVDL-005 Curcumin $[\mu M]_{eq}$, (iii) Determined average Fe^{2+} -TPTZ [µM] for each sample using the Fe^{2+} -TPTZ [µM] standard curve. (iv) % Antioxidant capacity of PVDL Veh, PVDL-005, N-acetylcysteine (NAC), gallic acid and ascorbic acid relative to 125[µM] curcumin.

3.4 Optimization of THP-1 adherence & macrophage differentiation

Phorbol 12-mytistate 13-acetate (PMA) triggers activation of non-adherent THP-1 monocytes to adhere and differentiate into macrophages[20]. The literature has no *a priori* information that standardizes the dose or duration of PMA for THP-1 macrophage differentiation. To establish an optimal dose and time of PMA exposure for QAC testing, that is sufficient—without being an excess stimulus but achieves monocyte to macrophage differentiation, we explored both dose and time effects following PMA exposure in 96-well culture plates. Cells (15,000) were initially seeded with PMA in 96-well plates and allowed to adhere and differentiate for either 16hr or 48hrs. The media was transferred to a new 96-well, thus transferring any non-adherent monocytes.

Monocytes retain a circular morphology with little to no filopodia, even if transiently adhered to cell culture plates (Fig-9Ai). Differentiation of macrophages assumes an irregular shape (Fig-9Aii) and are identifiable by their filopodia when fully differentiated (Fig-9Aiii) for phagocytosis [50]. Some THP-1 human monocytes adhered to cell culture 96-well plates even in the absence of PMA (Fig-9B/C retained). THP-1 monocytes that did not adhere, will continue to proliferate (Fig9B/C transferred). Surprisingly, the ethanol vehicle used in dissolution—when given at an amount proportional to that used in the highest concentration of PMA (vehicle of 2% ethanol)—also caused most cells to become adherent (Fig-9B/C, vehicle for 16hr/48hr). Almost all THP-1 adhered in the presence of PMA, regardless of dose, and this led to comparable levels of adhered macrophages (retained) at 16 and 48hr of PMA exposure and very low levels of non-adherent cells (transferred). However, not all macrophages show comparable cell metabolic activity with the same dose and duration of PMA. From 5-50[nM] for 16hrs, exposure to PMA had no appreciable effects compared to the untreated retained cell control (touched control) (or even an untransferred control well left untouched after seeding as a reference control) but metabolic activity started to decline from 50-200[nM] after 16hrs. After 48hrs of PMA exposure, 5-10[nM] had no appreciable effects compared to the vehicle control, whereas 25-200[nM] showed declining activity. Taken together, the optimal dose

of PMA was determined to be 10[nM] added to the media in which cells are seeded, as this ensures both adherence and differentiation with a good margin of tolerance.

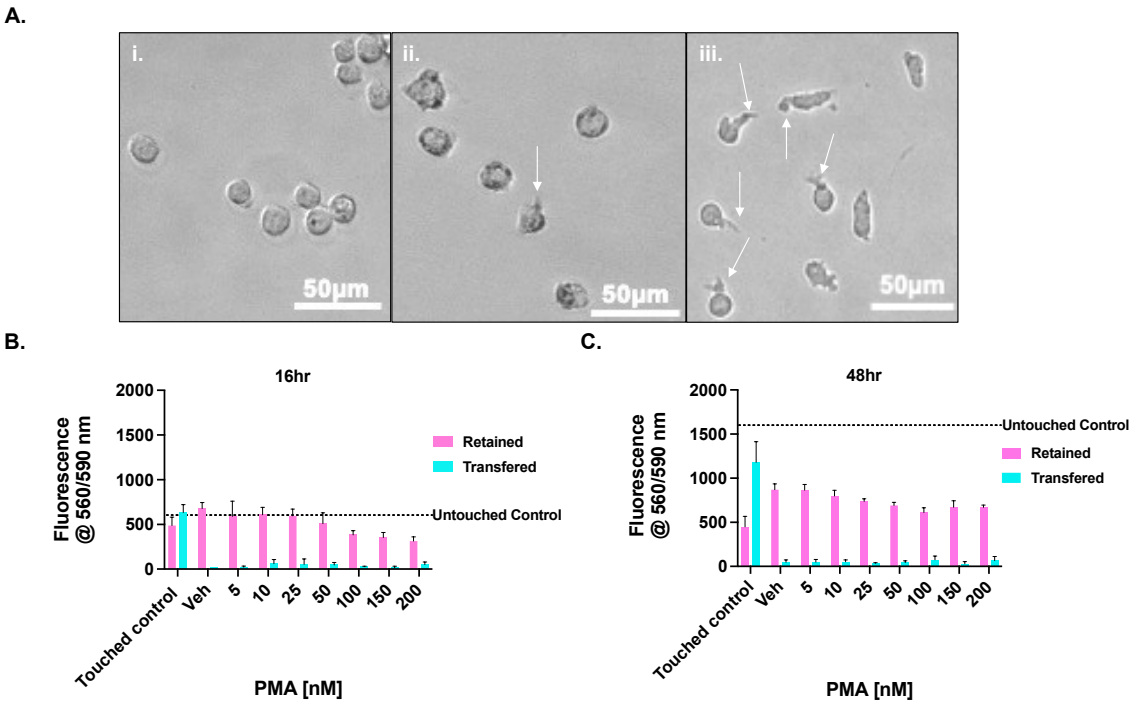

Figure 9: ***Concentration dependence of PMA stimulated adherence and differentiation of macrophages from non-adherent human monocytes.***

A) Non-adherent THP-1 cells (15,000) seeded onto 96-wells spontaneously adhere partly but show augmented adherence and differentiation evidenced by filopodia with PMA stimulation. i) monocytes without PMA; ii) macrophages exposed to PMA ethanol veh (2%, the equivalence of 200nM PMA) for 16hr; iii) macrophages exposed to 10nM PMA for 16hr (0.1% ethanol veh equivalent composition). Arrows indicate filopodia. Dose effect of PMA on cell adherence (retained) relative to non-adherent transferable cells after B) 16hrs and C) 48 hrs. Y-axis represents absolute fluorescence readings at 560/590nm after 1hr incubation with PrestoBlue cell viability reagent. All data was reported as absolute fluorescence 560/590nm for simplicity.

3.5 Effect of curcumin and PVDL-005 on HMOX1 protein

Induction of HMOX1 by 5[μM] curcumin is time dependent (Fig-10 A). Curcumin's induction of HMOX1 is highest at 6hr, but this effect abates with time, returning to baseline after 48hrs. Hemin is an FDA approved drug for the treatment of porphyria and, through the effect of inducing HMOX1 has the potential for anti-oxidative effects. THP-1 human macrophages treated with equivalent doses of curcumin [5μM] and hemin [5μM] show comparable induction of cytoprotective HMOX1 at 6hr (Fig-11A). The primary transcription factor purported to transactivate the HMOX1 promoter to induce expression by curcumin is Nrf2, which translocates to the nucleus after being phosphorylated. At an equivalent dose, curcumin and PVDL-005 did not increase phosphorylated-Nrf2 (p-Nrf2) levels compared to control or vehicles (Fig-12Ai). However, when comparing PVDL-005 to an equivalent amount of curcumin, the nanoparticle induced, significantly (2-fold) more HMOX1 by 6hrs (Fig-12Aii). THP-1 macrophages treated with $[5\mu M]_{eq}$ PVDL-005 for 6hrs showed a greater induction of HMOX1 compared to an equal dose of curcumin, suggesting that THP-1 macrophages may have accumulated more curcumin via PVDL-005 compared to its pure drug counterpart.

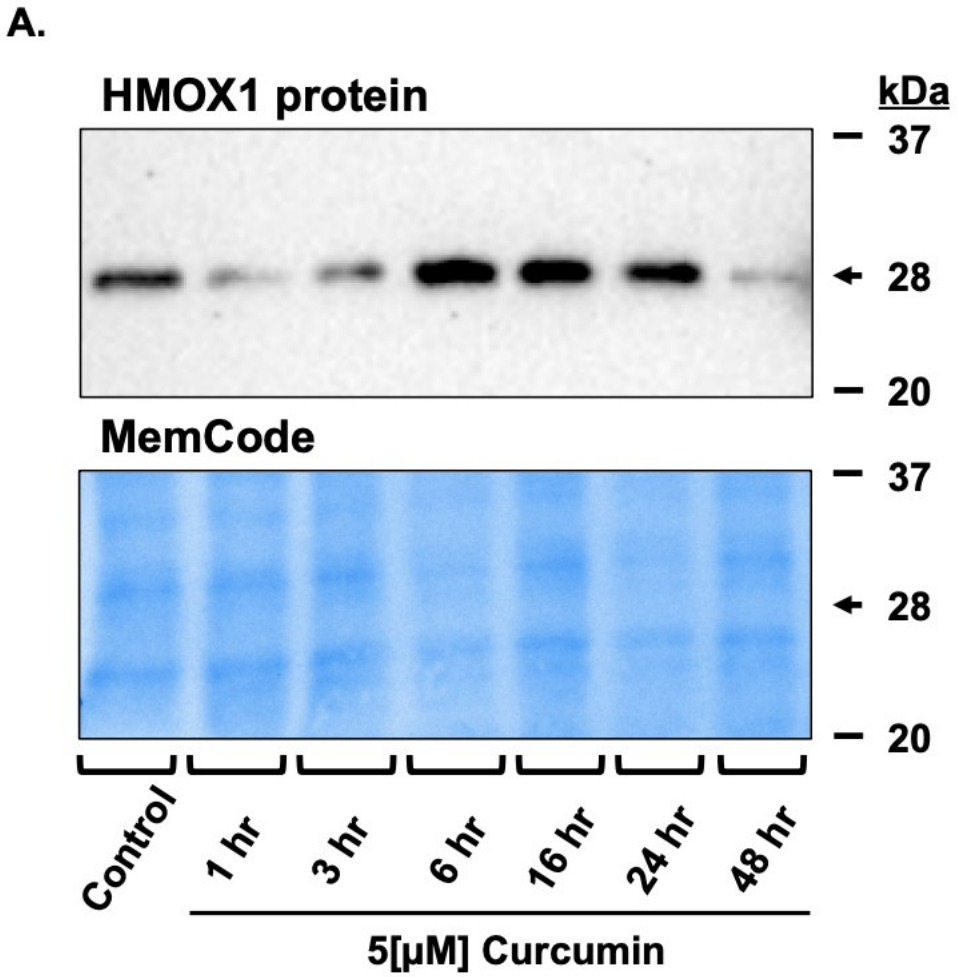

Figure 10: ***Time dependent induction of HMOX1 by curcumin.***

A) Immunoblot for HMOX1 protein expression *(~28kDa)* in THP-1 human macrophages treated with 5[μM] curcumin peaks at 6hr but the effect decreases from 16-48 hr. B) *Pierce® MemCode staining demonstrated uniform protein loading on the membrane prior to antibody probe.*

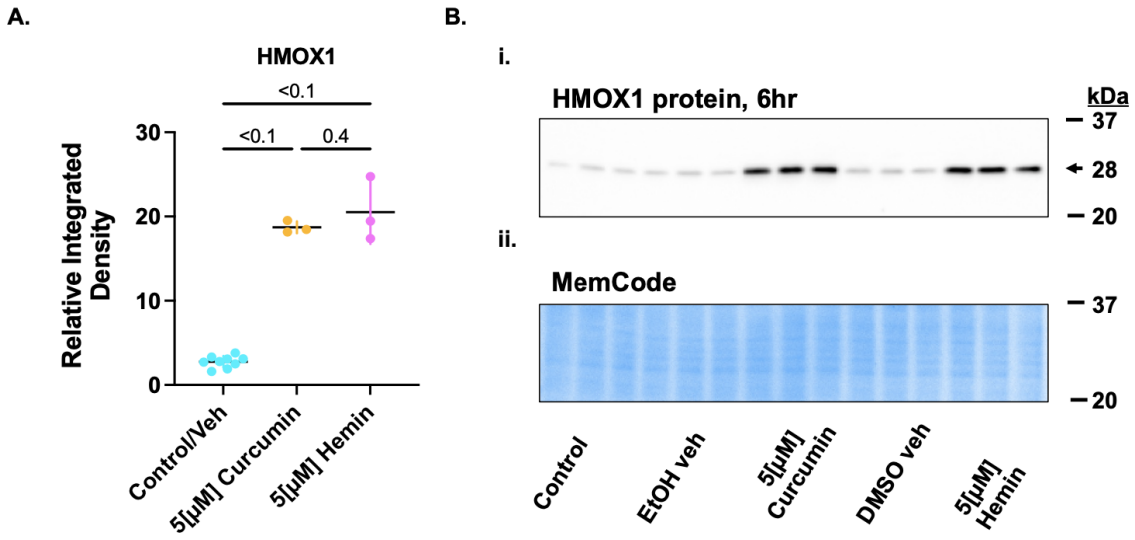

Figure 11: ***Curcumin & Hemin elicit equal dose-effect HMOX1 induction in THP-1 human macrophages.***

A) 5[μM] curcumin and hemin treated macrophages show equivalent activation of HMOX1 at 6hr (ns, P>0.05). Control and veh pooled together. (i) Representative HMOX1 probed membrane displayed specific HMOX1 bands at 28 kDa. (ii) Pierce® MemCode staining demonstrated uniform protein loading on the membrane prior to antibody probe.

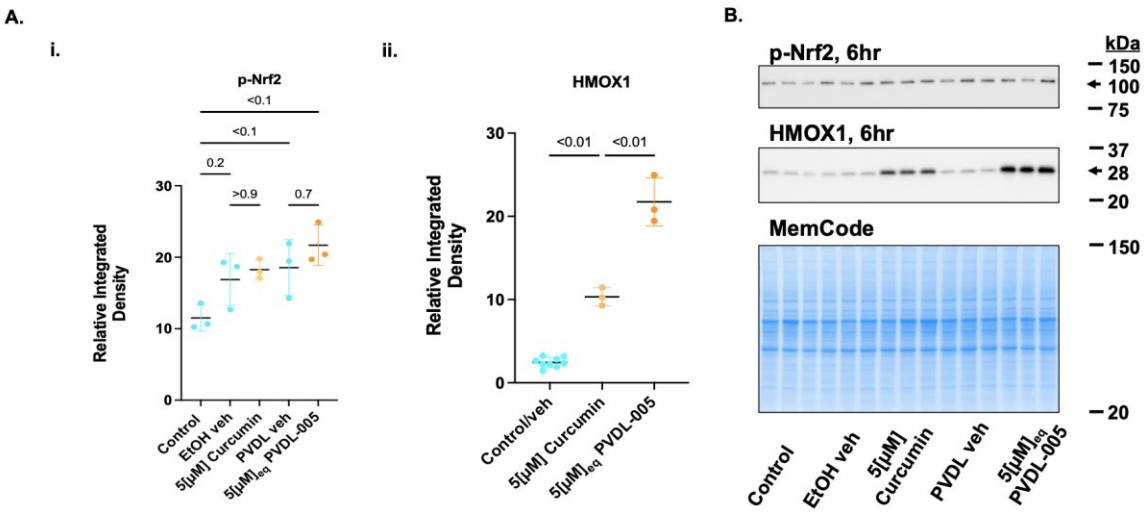

Figure 12: ***THP-1 human macrophages treated with a curcumin equivalent of PVDL-005 induce more HMOX1.***

Human macrophages treated with equal doses of curcumin and PVDL-005 show A) (i) no significant induction of p-Nrf2 ($P > 0.05$) but A) (ii) significant induction of HMOX1, where PVDL-005 causes greater induction of HMOX1 than curcumin. B) Representative p-Nrf2 and HMOX1 probed membrane displayed specific p-Nrf2 and HMOX1 bands at 100 and 28 kDa, respectively. Pierce® MemCode staining demonstrated uniform protein loading on the membrane prior to antibody probe.

3.6 Cellular uptake and internalization of PVDL-005

Human macrophages treated with nanoparticles of curcumin (PVDL-005, 5[μM]$_{eq}$) localized to the cytoplasm and nucleus of THP-1 human macrophages after 6hrs (Fig-13). FACS analysis was utilized to compare the degree of internalization between PVDL-005 and curcumin, (Fig-14). After 6hrs, there was a dose dependent difference between 2.5[μM] & 5[μM] curcumin (Fig-14 B) 45.6% and 148% increased intensity over vehicle treated cells, respectively. After 6hrs, there was a dose dependent difference between 2.5[μM]$_{eq}$ & 5[μM]$_{eq}$ PVDL-005 (Fig-14 C), 136% and 400% increased intensity over vehicle treated cells, respectively. Compared to an equivalent dose of 5[μM] curcumin, PVDL-005 had greater (+90%) fluorescent bioaccumulation of curcumin (Fig-14 D). Taken together, despite molar equivalence of curcumin, PVDL-005 showed a higher uptake efficiency of curcumin, possibly due to bulk phagocytosis. This could explain in part the higher proportional induction of HMOX1.

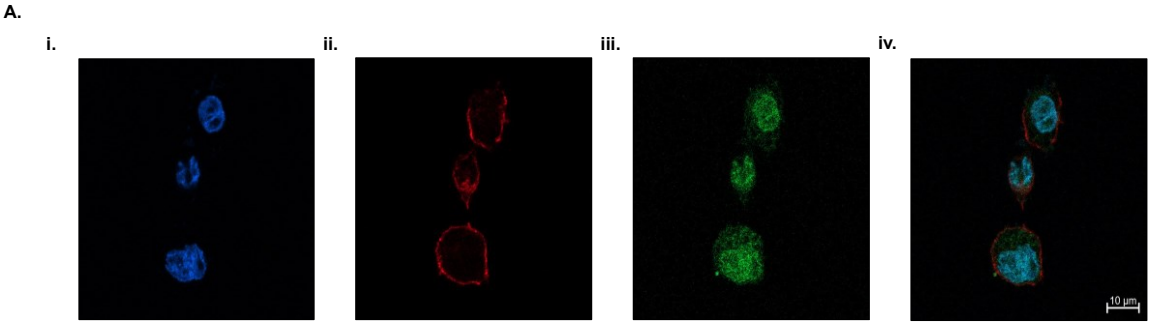

Figure 13: ***THP-1 human macrophages uptake of PVDL-005.***

Cytochemistry fluorescence of A)(i) Nucleus (Hoechest, blue), (ii) F-actin (Phalloidin, red) (iii)Curcumin (green) with (iv) Merged images of three previous panels.

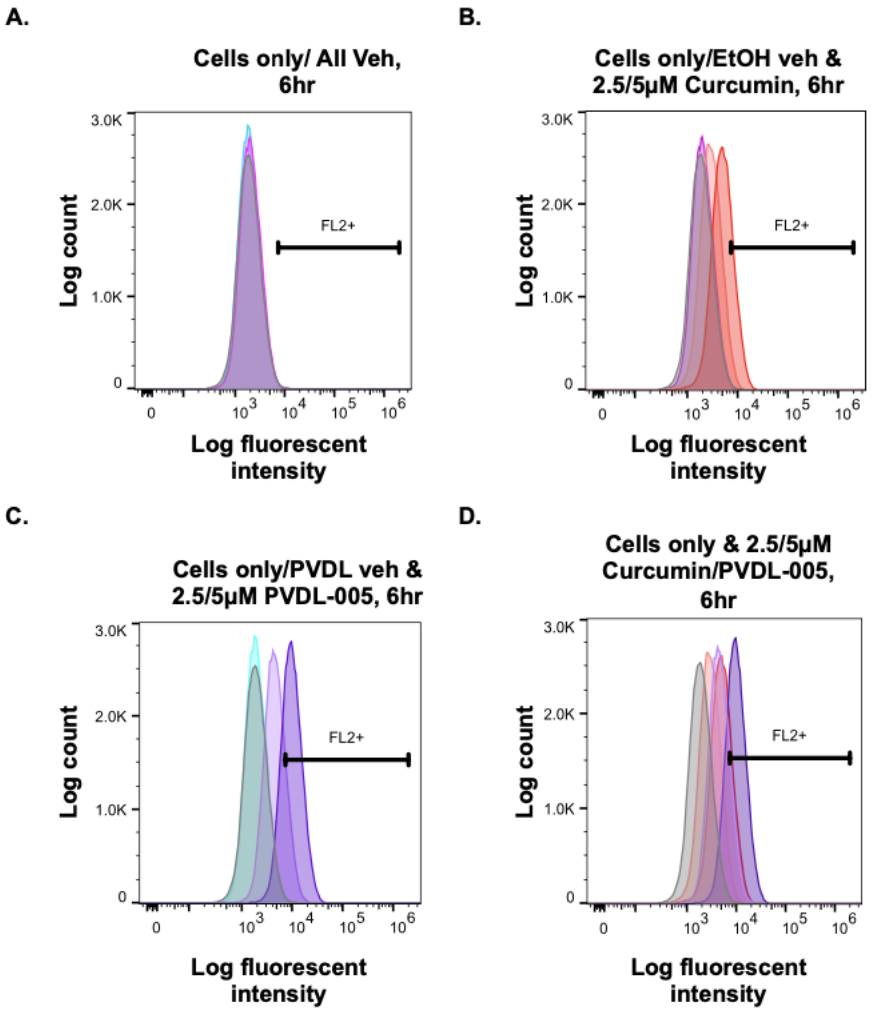

E.

Marker	Treatment group	% Total	Median
	Cells only	90.1	1923
	EtOH veh	89.6	2045
	PVDL veh	93.5	1929
	2.5[μM] Curcumin	90.5	2979
	5[μM] Curcumin	89.2	5070
	2.5$[\mu M]_{eq}$ PVDL-005	90.3	4549
	5$[\mu M]_{eq}$ PVDL-005	89.4	9661

Figure 14: ***Uptake of curcumin or PVDL-005 was determined after THP-1 cell isolation for Fluorescent Activated Cell Sorting (FACS) Flow Cytometry.***

Histograms in the FL2 (yellow/green) channel, with X-axis representing the log fluorescent intensity after 6hr of A) cells untreated or treated with vehicles (EtOH and PVDL veh) only; B) vehicle treated cells or 2.5 and 5[μM] curcumin; C) untreated and nano-vehicle treated cells or 2.5 and 5$[\mu M]_{eq}$ PVDL-005 treated cells, and D) untreated cells or 2.5 and 5[μM] curcumin or 2.5 and 5$[\mu M]_{eq}$ PVDL-005. Total number of events was 75,000cells; gating analysis was >65,000 cells, with ~90% gated (% total of total events counted). E) Tabulated values of each treatment group, % total of cells counted and absolute median fluorescent intensity.

3.7 THP-1 Macrophage dose response to curcumin and PVDL-005

The effect of fetal bovine serum (FBS) on THP-1 human macrophage viability was investigated as later assays involved lowering FBS levels prior to drug treatment to avoid interference with the interpretation of drug effects. Macrophages maintained their metabolic activity and viability in low FBS media for up to 30hrs (Fig-15 A). The data shows that low FBS media is well tolerated by THP-1 macrophages. It remains unclear why FBS when titrated down, caused a slight increase in metabolic activity, though we cannot rule out the potential for cell proliferation driven by autocrine signalling that was repressed by factors in FBS, distinct from metabolic activity.

FBS is a rich source of many growth factors and bioactive molecules and is typically associated with an ability to offset oxidative stress through receptor kinase signaling[51]. QAC methods that rely on safety and efficacy are best performed in chemically defined media to avoid FBS batch and lot variability that can interfere with reproducibility. To determine how FBS levels might alter methods of analysis for cytoprotection, the tolerance to H_2O_2 a potent pro-oxidant that increases ROS was tested. Interestingly, H_2O_2 was more toxic to THP-1 human macrophages conditioned to high (10%) FBS (Fig-16 A) supplemented media compared to low (0.5%) FBS (Fig-16 B). Macrophages were highly resistant to oxidative stress due to H_2O_2 with LD_{50} of 1.1[mM] (high FBS) and 2.1[mM] (low FBS).

It was a surprise to learn that curcumin had a narrow treatment window, with LD_{50} of 10.7[μM] (high FBS) and 6.9[μM] (low FBS) (Fig-17 A and B). Curcumin compared to H_2O_2 was less well tolerated, and high FBS offered additional protection against the toxic effect of curcumin. Interestingly, PVDL-005 had a wider safe treatment window (LD_{50} of 10.3[μM]$_{eq}$) compared to PVDL-004 (8.2[μM]$_{eq}$) in low FBS treated macrophages (Fig-18A and B). These two nanoparticle formulations differed only in the liquid vehicle excipient used. PVDL-005 (i.e., ethanol + saline solution as excipients) was selected as the primary formulation of interest due to equivalency and safety to curcumin and PVDL-004

(i.e., bovine serum + saline solution as excipients) for comparison. This could be an effect also of molecular corona on the nanoparticles and requires further investigation.

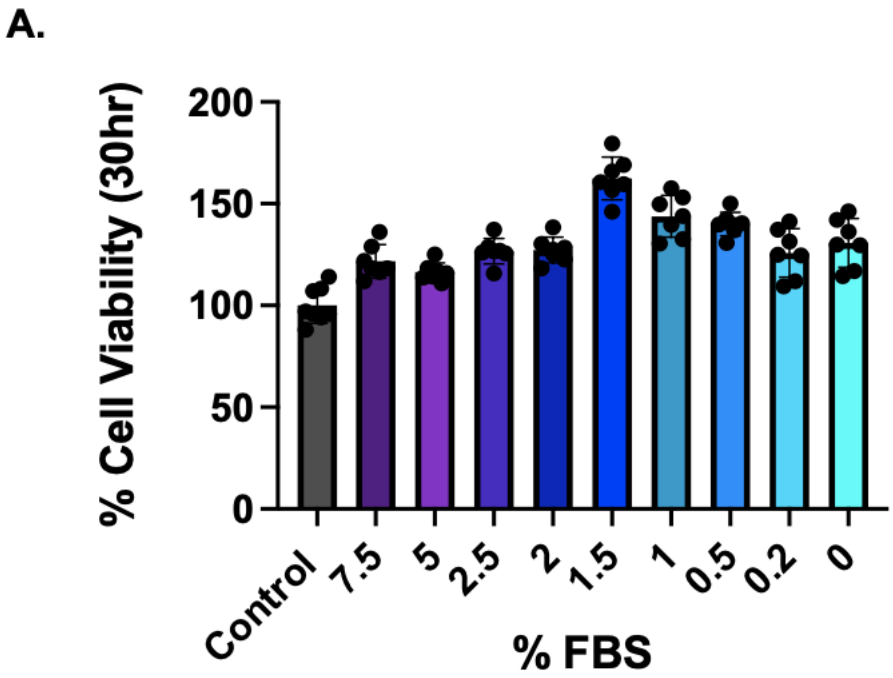

Figure 15: ***THP-1 human macrophages maintain high viability in FBS reduced media.***

Viability of THP-1 human macrophages in media with titrated FBS levels. Data normalized to control. Control was 10% FBS media.

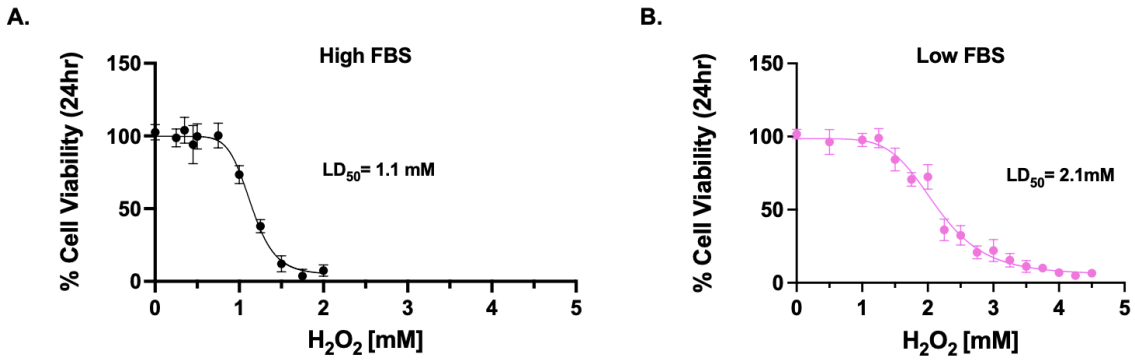

Figure 16: ***Effect of FBS on macrophage tolerance to H_2O_2.***

Human macrophages treated with H_2O_2 at various concentrations for 24hrs to establish a viability curve and LD_{50} with, A) High, 10% FBS, LD_{50}=1.1[mM] and B) Low, 0.5% FBS, LD_{50}=2.1[mM]. Data is normalized to a media-only control.

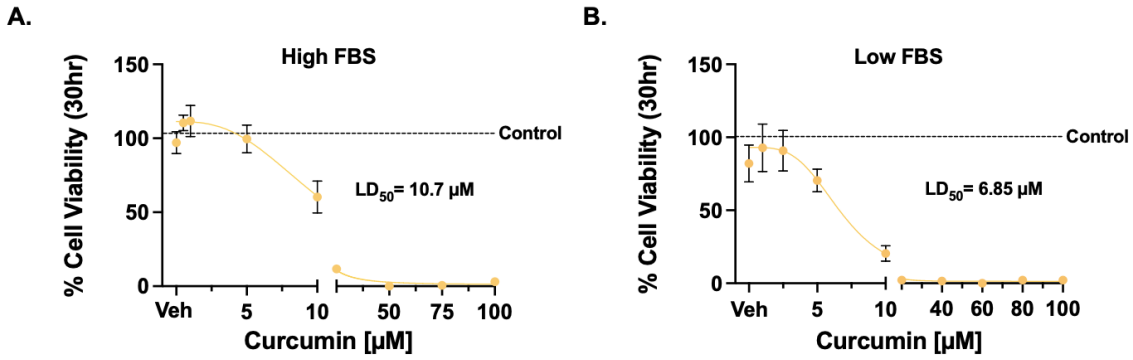

Figure 17: ***Effect of FBS on macrophage tolerance to curcumin.***

Curcumin viability curve at A) High, 10% FBS, LD_{50}=10.7[µM] and B) Low, 0.5% FBS, LD_{50}=6.85[µM]. Data is normalized to a media-only control.

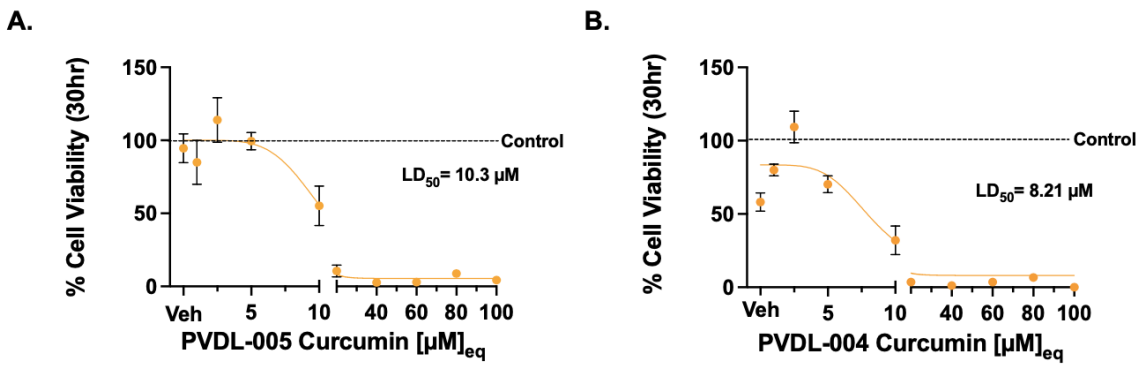

Figure 18: ***Macrophage tolerance to PVDL nanoparticles.***

Dose response curves for A) PVDL-005, LD_{50}= 10.3[µM] and B) PVDL-004, LD_{50}=8.21[µM]. Data is normalized to a media-only control. Assay performed in low FBS conditions.

3.8 The cytoprotective potential of PVDL-005

To further determine how FBS levels might alter methods of analysis for cytoprotection, the nanoparticle liquid vehicle excipients were tested in the presence of high (10%) and low (0.5%) FBS media as indicated for the pre-treatment experimental design (Fig-19 A). There was significant cytoprotective effect after a 6hr pre-treatment of 2.5[μM]$_{eq}$ ethanol + saline solution (i.e., liquid vehicle excipient for PVDL-005) followed by H_2O_2 for 24hrs, in high FBS supplemented media conditions (Fig-20 A, $P<0.01$). In low FBS conditions, a 6hr pre-treatment of 100/20[μM]$_{eq}$ bovine serum + saline solution (i.e., liquid vehicle excipients for PVDL-004) did not offer any additional cytoprotection with H_2O_2 (Fig-20 B, $P=0.06$ and $P=0.92$), but 100[μM]$_{eq}$ bovine serum + saline solution in absence of H_2O_2 lowered cell viability (Fig-20 B, $P<0.01$). There was no evidence of cytoprotection from a 6hr pre-treatment of 100/20[μM]$_{eq}$ ethanol + saline solution (liquid vehicle excipients for PVDL-005) with H_2O_2 relative to the H_2O_2 CTRL in low FBS supplemented media conditions (Fig-20 C, $P=0.26$ and $P=0.29$), and 100[μM]$_{eq}$ liquid vehicle excipient without H_2O_2 was well-tolerated by macrophages (Fig-20 C, $P=0.20$). The cytoprotection assays (shown in later section) involved treating THP-1 human macrophages with PVDL-005 in the presence of H_2O_2. This prompted the adjustment of the composition of FBS in the media prior to treatment to limit potential unknown interactions between compounds found in FBS and our nanoparticle liquid vehicle excipients (ethanol + saline solution) in the presence of H_2O_2. By lowering serum levels in media, any potential cytoprotective effect would likely be due to curcumin or turmeric nanoparticles and not FBS. Further, 0.5% was the FBS composition goal for testing due to evidence of its use with THP-1 macrophages [52–54] and because these cells maintained viability in low serum media for at least 30hrs, which is the duration of our experimental design.

Given that curcumin was shown to induce cytoprotective HMOX1 levels in macrophages, its anti-oxidant potential in the presence of H_2O_2 was investigated. In our previous studies, 2.5[μM] was found to be a safe dose of curcumin, while 5[μM] curcumin led to a decrease in cell viability. We elected to investigate the

cytoprotective potential at both 2.5[μM] and 5[μM] curcumin in the presence of H_2O_2 to maintain consistency in dosing with PVDL-005 (i.e., safe at $2.5[\mu M]_{eq}/5[\mu M]_{eq}$) shown in later sections. 6hr pre-treatment of 15[mM] NAC (i.e., positive control) but not 2.5/5[μM] curcumin, was cytoprotective ($P<0.01$) against H_2O_2 in THP-1 human macrophages (Fig-21 A). Although our previous studies showed 2.5[μM] curcumin was well tolerated, a 6hr pre-treatment of the vehicle ($2.5[\mu M]_{eq}$ lowered cell viability (Fig-21 A, $P<0.01$), which may be due to inter-assay variability. Interestingly, the pre-treatment of 2.5/5[μM] curcumin lowered macrophage viability relative to the H_2O_2 CTRL and vehicles.

Despite curcumin's inability to achieve cytoprotection by pre-treatment, PVDL-005 cytoprotective potential was investigated as it showed greater induction of cytoprotective HMOX1 compared to curcumin. Simultaneous treatment of PVDL-005 with H_2O_2 did not confer any cytoprotective benefit to THP-1 human macrophages (Fig-22 A). Pre-treatment of PVDL-005 $2.5[\mu M]_{eq}$ and $5[\mu M]_{eq}$ for 6hrs (Fig-22 B) was not cytoprotective against H_2O_2. Again, the pre-treatment of $5[\mu M]_{eq}$ PVDL-005 (nanoparticle of curcumin) (Fig-22 B) lowered cell viability compared to H_2O_2 CTRL and vehicles. To ensure that there was no concurrent stress from curcumin and H_2O_2, we investigated also whether macrophages could benefit from lower doses (i.e., $0.5[\mu M]_{eq}$ and $1[\mu M]_{eq}$) of PVDL-005 for a longer duration of time. However, pre-treatment of PVDL-005 using $0.5[\mu M]_{eq}$ and $1[\mu M]_{eq}$ for 24hrs was also not cytoprotective against H_2O_2 (Fig-22 C). Yet, a 24hr pre-treatment of 15[mM] NAC was cytoprotective (Fig-22 C, $P<0.01$), similar to how NAC was previously shown to be protective with 6hr pre-treatment (Fig-21 A).

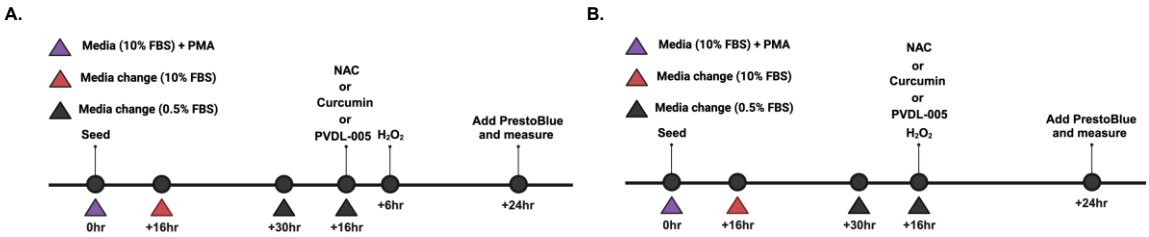

Figure 19: ***Cytoprotection assay experimental design.***

(A) 6hr pre-treatment of Curcumin/PVDL-005/NAC followed by H_2O_2 for 24hrs (total assay time of 30hrs) and (B) simultaneous treatment of H_2O_2 and NAC/Curcumin/PVDL-005 for 24hrs with PrestoBlue incubation (1hr). All cells are conditioned in 0.5% FBS for 16hrs prior to drug or H_2O_2 treatment**.**

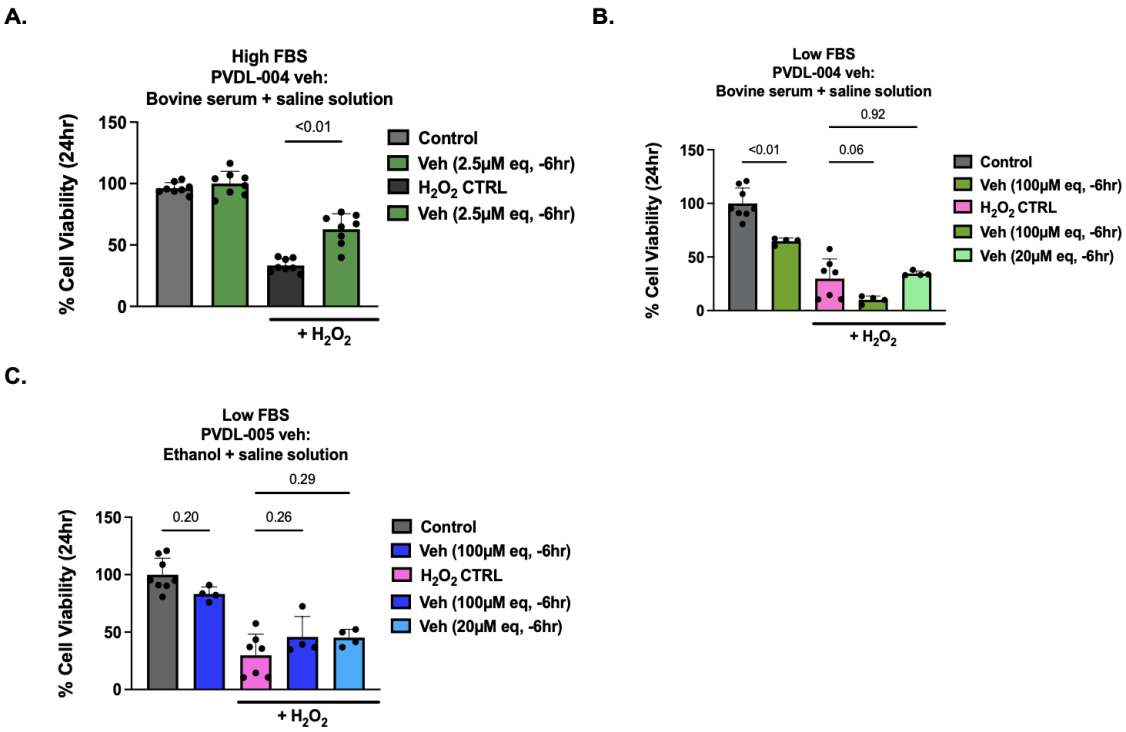

Figure 20: ***Cytoprotective effect seen with nanoparticle excipients at high FBS but not low FBS conditions.***

6hr pre-treatment of nanoparticle liquid vehicle excipients followed by H_2O_2 for 24hrs shows cytoprotective effect in THP-1 macrophages at A) High FBS conditions, but not B)/C) Low FBS conditions. The H_2O_2 [mM] used at high and low FBS were 1.1[mM] and 2.1 [mM], respectively. Data normalized to control.

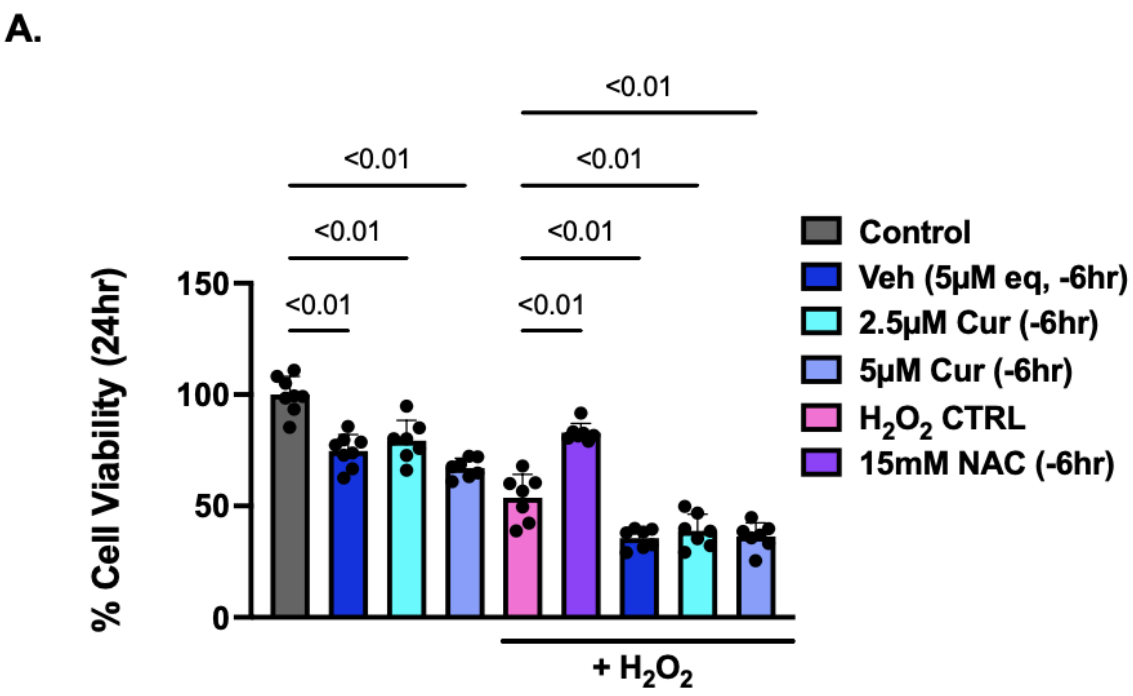

Figure 21: ***Curcumin prophylaxis treatment did not confer cytoprotection to macrophages in vitro.***

A) Pre-exposure of curcumin at 2.5 or 5 [μM] for 6hrs in a low FBS condition prior to oxidative stress challenge by H_2O_2 (2.1mM). Data normalized to a media-only control.

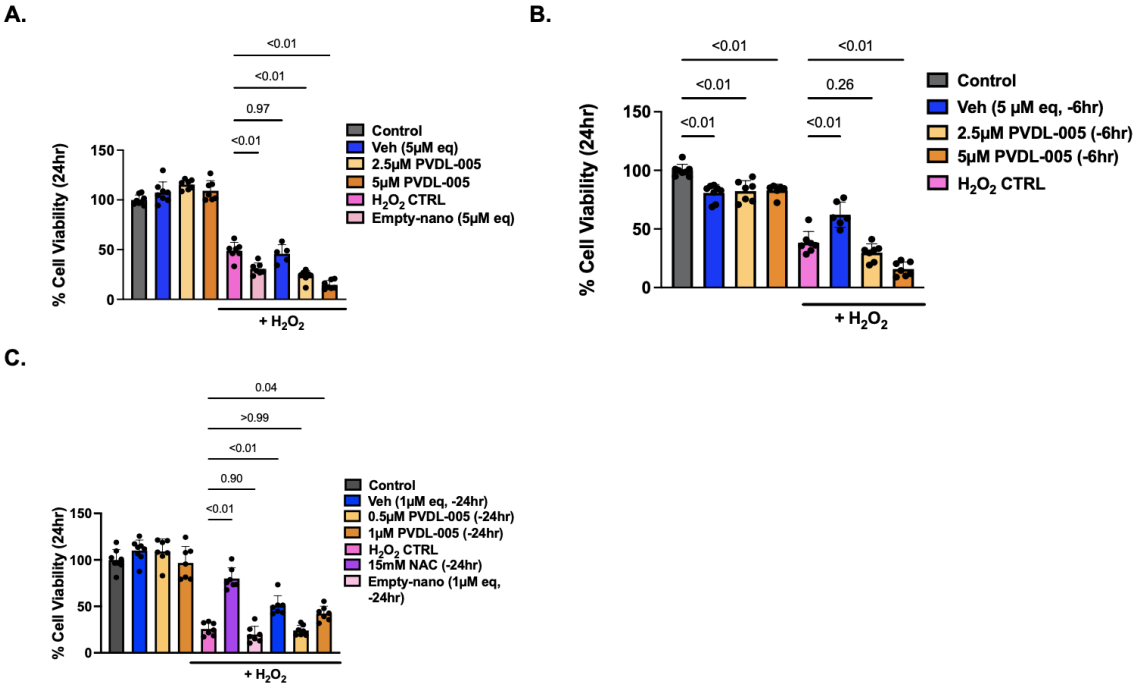

Figure 22: ***Nanoparticle formulation of curcumin (PVDL-005) by prophylaxis or simultaneous dosing conferred no cytoprotection to macrophages in vitro.***

A) Exposure of PVDL-005 at 2.5 or 5 $[\mu M]_{eq}$ immediately followed by H_2O_2 (2.1[mM]) had no effect compared to vehicles or benefit compared to H_2O_2 alone in low FBS conditions. B) Pre-emptive exposure of PVDL-005 at 2.5 or 5 $[\mu M]_{eq}$ for 6hrs, followed by H_2O_2 (2.1[mM]) had no effect compared with vehicles or benefit compared to H_2O_2 alone in low FBS conditions. C) Pre-emptive exposure of PVDL-005 at 0.5 or 1 $[\mu M]_{eq}$ for 24hrs, followed by H_2O_2 (2.4[mM]) had no effect compared with vehicles or benefit compared to H_2O_2 alone in low FBS conditions. Data normalized to media-only control.

Chapter 4: Discussion

4.1 Summary of findings

Here we have characterized the biophysical properties of turmeric root extracted botanical nanoparticles (PVDL-005 nanoformulation) and established the analytical, reference-based QAC methods and reference data required for good manufacturing practices (GMP) or chemistry manufacturing controls for nano-pharmacology—to advance further *in vitro* and *in vivo* equivalency studies (i.e., using curcumin as reference). The PVDL-005 nanoformulation is a uniform, stable colloidal solution of spherical nanoparticles with a consistent hydrodynamic size (177nm) and a neutral surface charge. We established a chemical-reference based: determination of molar equivalency (soluble curcumin), total antioxidant capacity (FRAP), and equivalency (FACS uptake & HMOX1 induction) of the PVDL-005 formulation. We determined an approximate empty nanoparticle control of similar botanical biophysical properties to PVDL-005 devoid of API, though not of biological effect. We established that PVDL-005 showed enhanced uptake and induction of HMOX1 in human macrophages. We determined the safety and tolerability of PVDL-005 to establish a therapeutic range in human macrophages. PVDL-005 has an improved safety profile (LD_{50}=10.3[μM]$_{eq}$) than solubilized curcumin (LD_{50}=6.9[μM]) in human macrophages. Finally, curcumin nor PVDL-005 at the dose or timing tested were protective to macrophages in the presence of H_2O_2. Further investigations into the efficacy of PVDL-005 for inflammatory regulation and additional pharmacological characterization are warranted.

4.2 Importance of biophysical and chemical QAC

The characterization of PVDL-005 size, shape and surface charge (i.e., by zeta potential) of nanoparticles is required to meet regulatory guidelines set by the FDA[55]. A high nanoparticle density (1X) means that the nanoparticles are in proximity and tightly packed. This may cause the DLS instrument to read two or three nanoparticles as one. As such, it is important to dilute nanoformulations to

establish a low-density colloidal solution of nanoparticles that is stable, regardless of further dilution (5X, 10X and 15X). This explains why the differential in the average hydrodynamic size between 1X compared to 5X, 10X and 15X. However, in order to determine shelf-stability for GMP, at least 13-weeks of shelf-life storage at various temperatures is expected (50^{o}C, 22^{o}C, & 8^{o}C), thereafter the dynamic light scatter can be repeated to ensure that the particles have not aggregated or fused/flocculated (EMA, CPMP/ICH/2736/99). Nanoparticles with zeta potentials that are between +30mV and -30mV are at greater risk for aggregation [56]. We stored nanoformulations for up to four months under refrigeration (~4-8C) and observed no change in hydrodynamic size or zeta potential. Further research should evaluate drug stability over time (at least 1 year). PVDL-005 nanobotanicals are extracted from turmeric biomass and could contain a heterogenous mixture of curcumin and other compounds. Interestingly, derivatives of curcumin like desmethoxycurcumin and bisdemethoxycurcumin dissolved in ethanol have been shown to absorb light at 419 and 424nm, respectively [57]. This slightly deviates from the 430nm absorption peak used here for curcumin and PVDL-005 referencing. As such, we did not rule in or out these additional curcumin derivatives in our PVDL-005 nanoformulation, which could influence the equivalency and efficacy. Moreover, the commercial reference of curcumin was adjusted for purity from the specification sheet, as it was not 100% pure analytical grade. Future, studies, should validate the molar equivalence in the reference and formulated nanoparticles for absolute curcumin, curcumin derivatives, or curcumin metabolites by liquid chromatographic mass spectrometry.

4.3 THP-1 macrophages as a model cell line for nanoparticles

THP-1 are an ideal initial cell line to work with for determining nanoparticle equivalency (i.e., using curcumin as reference), as they have the capacity, once differentiated to macrophages, to naturally phagocytose nanoparticles. They also serve to model macrophages of the reticuloendothelial system *in vivo*, where nanoparticles are likely to accumulate depending on the route of administration

(eg., *i.v., i.p.* or *p.o.*)[58,59]. These cells are also less likely to be impacted—favourably or not—by the surface charge of nanoparticles due to their inherent phagocytotic properties. These cells are also excellent models for evaluating inflammation and cytoprotection directly or indirectly (for example if conditioned media is collected for transfer to other cells for paracrine effect analysis). However, notable differences in the stoichiometry of the number of cells to the volume of media in expansion 100mm plates, 35mm dishes, and 96-well plates should be considered when optimizing methods. For example, it was observed that 5[nM] was insufficient to maintain adherence for cell lysate collection in western blotting compared to 10[nM] PMA. Since there was comparable viability, 10[nM] was selected instead of 5[nM] PMA for all in vitro experiments. The previously reported concentrations of PMA used to achieve THP-1 differentiation is highly variable and ranges from 8[nM]-600[nM] anywhere from 1-5 days incubation, which presents a challenge in selecting an appropriate dose for differentiation[60]. Our PMA optimization experiment covered a dose range of 5[nM]-200[nM] for 16-48hrs, which were most commonly reported dose and time boundaries[61–64]. In this experiment the transferred media would also contain PMA, and so likely also caused the transferred cells to adhere and differentiate. Monocytes that were in the control transferred well would likely continue proliferating over duration of the experiment (48hrs). Our data suggest that PMA exposure might also limit/halt cellular proliferation. Future studies should explore and confirm the impact of PMA on THP-1 cell cycle. The untouched control reading should be the sum of the control retained and the control transferred, but seeding error or proliferation may explain why this was not the case. Future determinations could be made more accurate by utilizing cell cycle inhibitors or no-serum when testing adherence and differentiation. Also, the presence of filopodia is not a robust confirmation of monocyte-to-macrophage differentiation and does not determine the polarization of macrophages. Increases in CD68 and MHC II expression have been used to confirm monocyte-to-macrophage differentiation, and other markers could be further tested to confirm or determine polarization to either M1 or M2 phenotypes[65]. These THP-1 differentiated

macrophages were not exposed to any additional stimuli expected to elicit M1 or M2 polarization. Typically, THP-1 differentiated macrophages can be polarized to M1 or M2 using LPS with IFN γ or IL-4, respectively[20]. However, it is possible that drug treatments (i.e., curcumin, PVDL-005, hemin or H_2O_2) may have caused a release of autocrine and paracrine factors that might polarize macrophage phenotype to M1s or M2s. The differentiation and polarization of macrophages might impact the modification of their cytoprotective and inflammatory profiles in efficacy testing and inform future analyses.

Prior work with THP-1 macrophage cells have used low FBS composition before drug treatment or stimulus[52–54]. Variability in FBS and the amount used in studies could also contribute to challenges in consistency and reproducibility of *in vitro* data [21]. FBS can influence the stability of polyphenolic compounds (i.e., resveratrol analogues) through chemical polyphenol-protein interactions, where the final concentration of the compound is lower after incubation with FBS[66]. As such, lowering FBS levels may help with consistency by reducing, if not eliminating risk of potential interactions between curcumin and other constituents in media or effects of media constituents alone. Future approaches should condition cells to a defined animal/xenofree media that does not require FBS, thereby reducing uncontrolled variability[22,23]. Otherwise, minimal FBS or strategies that reduce the risk of interference (eg. heat inactivation) could be integrated into future protocols.

4.4 Identifying suitable excipients and nano-vehicles for PVDL-005

There are limitations of not having a true empty-nanoparticle control, as would be expected with synthetic processes of developing nanocarriers for active pharmaceutical ingredients. Classically, with drug-loaded nanoparticles, the drug and the nanoparticles are two separate entities that are combined sequentially in the process of forming the nanodrug. This allows for ready access to an empty-nanoparticle vehicle for use in biological assays as a control for the drug-loaded nanoparticle. Extraction of turmeric nanoparticles from the turmeric root meant that curcumin and the nanoparticle were inseparable, as they were formulated as

a singular entity by the extrusion process. Unlike synthetic nanoparticles that are drug-loaded, our derivative nanoformulation is considered a botanical, and so too has the added challenge of comparing effects to a presumably inert nano-vehicles devoid of API. Extraction of similar nanobotanical from plant material devoid of API using parallel botanical processes might provide an option. The FDA has released guidance on botanical formulations (FDA-2000-D-0103), which present an opportunity for nano-botanical classification distinct from nonbotanical nanomedicines (FDA-2017-D-0759). Regardless, it is important to control for colloidal effects of excipients and nano-vehicles distinctly from the API of the botanical, as opsonization and other corona protein (i.e., formation of plasma protein layers on the surface of nanoparticle) modification can impact stability, safety, efficacy (i.e., targeting efficiency), and tolerogenicity (FDA-2017-D-0759). Human plasma/serum has not yet been tested on these formulations, nor have we evaluated the nano-botanicals for any protein corona influences, but this would be an important future step to developing a final formulation for pre-clinical study or clinical testing.

Identifying an appropriate nanoparticle control was challenging. A not yet tested option that might be considered in future would be a deconstructed form of PVDL-005 into its lipid components, removing the curcumin/APIs by dialysis and then reforming the empty-nanoparticle. The downside risk however might be reduced integrity of the intrinsic lipid composition of the nanoparticle. Alternatively, an empty synthetic liposomal standard from a nanoparticle production facility could be used. The alternative approach that was used here acquired an approximated substitute as a close-to-control nano-vehicle, through a similarly processed extrusion of yeast. The synthetic option presents a challenge in that the empty nanoparticle is homogenous and not botanical (heterogenous) in lipid constituents. Thus, achieving a close-to-control, heterogenous botanical that is somewhat biologically inert as a nanoparticle control was determined to be the best approach. Additional studies of the composition of the botanical, including a detailed certificate of analysis, might allow for a close-to-control nano-vehicle to be made synthetically.

Nanobotanicals are a relatively new area of therapeutic development in a rapidly growing space of nanopharmacology; so regulators should provide additional direction compared to existing nanoparticle safety testing that combines the botanical and nanoparticle regulations/guidance.

4.5 The cytoprotective potential of curcumin vs nanocurcumin

PMID	Cell type	[Curcumin] Duration	HMOX1	Stressor	Results
Habiyambere *et. al* (This thesis)	Macrophage (THP-1; Hu)	0-5[μM]# -6hrs; -24hrs	↑	H_2O_2	n/c or ↓Viability ↑TAC; n/m ROS n/m Cytokines
33545894 [67]	Macrophage (RAW 264.7; Ms)	2.5[μM]# -24hrs	n/m	LPS; 24hrs	↓ Cytokines
31112588 [68]	Macrophage (RAW 264.7; Ms)	5-20[μM] -24hrs	n/m	H_2O_2; 4hrs	↓ ROS n/c Viability
27492022 [39]	Endothelial (Vein) (HUVEC; Hu)	2.7/14[μM]# 24hrs	n/m	H_2O_2; 24 hrs	↓ ROS-nanocur. n/c ROS- curcumin ↑Viability-curcumin n/c Viability-nanocur.
16953118 [40]	Epithelial (Blad.) (ECV304; Hu)	1-15[μM]^ -6hrs	↑	H_2O_2; 2hrs	↑Viability
27492022 [39]	Endothelial (Vein) (HUVEC; Hu)	2.7/14[μM]# 24hrs	n/m	H_2O_2; 24 hrs	↓ ROS-nanocur. n/c ROS- curcumin ↑Viability-curcumin n/c Viability-nanocur.
18001810 [69]	Epithelial (Lung) (RLE-6TN; Rat)	10[μM]# 24hrs	↑	DQ12; 24hrs	↑Viability
31530014 [70]	Epithelial (Lung) (A549; Hu)	200[μM]; -2hrs	n/m	Microbe; 24hrs	↑Viability
21857083 [71]	Hepatocytes (HepG2; Hu)	1-5[μM]; -24hrs	n/m	H_2O_2; 24hrs	n/c Viability
37411033 [72]	Epithelial (Lung) (BEAS-2B; Hu)	544[μM]# -12hrs	n/m	$PM_{2.5}$; 24hrs	↓ ROS ↑Viability-nanocur. n/c Viability-curcumin

Table 1 ***Summary of results from literature investigating the cytoprotective effects of pre-treatment or simultaneous administration of curcumin and nanocurcumin in different cell lines.***

[#] Nanocur (nanocurcumin) was included in the study; ^Curcumin and derivatives of curcumin were incorporated in the study. Hu=Humans, Ms=Mouse, blad=bladder, n/c=no change, n/m= not measured. TAC= Total Antioxidant Capacity, DQ12=Quartz (i.e., cytotoxic) and $PM_{2.5}$ = particulate matter $\leq$2.5µm (i.e., cytotoxic).

The THP-1 human monocytic cell line was isolated from a 1-year old male leukemia patient. As such, they are homogenous, stable and useful for modelling monocytes and macrophages, compatible with differential polarization to M1/M2-like cells[20]. However, the cell line is immortal due to its malignant origin, which presents a limitation compared to primary human monocytes. Curcumin has a well-established paradoxical effect on primary vs malignant cell types; and has shown to offer both cytoprotective and cytotoxic to different cells at the same dose. Curcumin's effects on cells are also influenced by its chemical modification/ derivatization (eg. demethylation) or encapsulation (eg. into nanoparticles). Moreover, as we showed in our findings, cytoprotection, neutral effects, or cytotoxicity are dose-dependent, which is consistent with prior literature and varies with cell type (also possibly by species), including macrophages (see Table-1, for summary). The benefit of curcumin is predominantly mediated by cell signaling resulting from the induction of heme-oxygenase-1 but it has also been shown to limit inducible nitric oxide synthase and cyclooxygenase-2. Collectively, this results in a reduction of reactive oxygen species (ROS) and generation of cytokines (eg. MCP-1/2, TNF α, IL-1, IL-6). Though some reports show an increase in ROS due to curcumin, they have also lacked adequate controls to account for the fluorescent nature of the drug[28]. Though we did not establish cytoprotection at the dose or timing tested, we have not explored all manner of benefits either (eg. metabolic, inflammatory). Prior studies have shown cytoprotection in the dose range we tested. For example, when RAW 264.7 macrophages were pre-treated with 5-10[μM] curcumin and exposed to H_2O_2 for 4hrs cell viability was increased (as determined by MTT assay) (Table-1). Nanocurcumin (curcumin encapsulated gold nanoparticles; AuNP-C) could safely be treated to doses up to 814$[\mu M]_{eq}$ in RAW 264.7 macrophages for 24hrs compared to 40 [μM] for curcumin (as determined by MTT assay)[73]. These findings suggest that nanoparticles of curcumin (AuNP-C) were less toxic to macrophages compared to unmodified curcumin[73]. Doggui *et al.* investigated the cytoprotective potential of nanocurcumin (curcumin encapsulated poly(lactide-co-glycoside) based-nanoparticulate formulation; Nps-Cur) and

curcumin in SK-N-SH human neuroblastoma cells[74]. They found that cells could only tolerate up to 0.1[μM]$_{eq}$ of nanocurcumin and 0.07[μM] curcumin for 24hrs (as determined by Lactate dehydrogenase (LDH) cytotoxicity assay). Simultaneous treatment of 0.07[μM]$_{eq}$ nanocurcumin, but not 0.07[μM] curcumin was cytoprotective relative to an H_2O_2 negative control[74]. They also demonstrated that SK-N-SH neuroblastoma cancer cells treated with 0.07[μM]$_{eq}$ nanocurcumin exhibited higher production of GSH (i.e., antioxidant metabolite) compared curcumin, relative to an H_2O_2 negative control, suggesting that nanocurcumin may have superior antioxidation potential[74]. The lowest dose we tested was 0.5[μM]$_{eq}$, so it may be that lower doses, if presumably able to be directly antioxidant or indirectly still induce HMOX1, could offer benefit. Future studies should look to examine a greater range curcumin for either direct or indirect efficacy. Ghoreyshi *et al.* determined 21[μM] and 125[μM]$_{eq}$ were tolerated doses for curcumin and nanocurcumin (encapsulated poly(lactic-co-glycolic) acid-chitosan-shield-folic acid nanoparticles; Curcumin-PLGA-CS-FA) in human U87-MG glioblastoma cancer cells, respectively (i.e., 24hr exposure, determined by resazurin assay)[75]. Cells treated with 125[μM]$_{eq}$ nanocurcumin exhibited low ROS production (i.e., determined by DCF-DA fluorescence) and promoted an increase in superoxide dismutase (SOD) and catalase (CAT) activity, which are enzymes known to regulate antioxidation in cells (i.e., results do not show comparison between nanocurcumin to curcumin for these sets of experiments)[75]. This finding that the nano-formulation of curcumin is safer compared to curcumin alone in glioblastoma cells suggests that the pharmacodynamics of a nanoformulation is also an important and determinant variable to tolerance or efficacy. This was confirmed in neuroblastoma cell lines (SMS-KAN, LA-N-6, IMR-32, SK-N-AS) that showed a low tolerance for 100 [μM]$_{eq}$ nanocurcumin (curcumin encapsulated dextran nanoceria; Dex-CNP-Cur nanoparticles) compared to 100[μM] curcumin after 24hrs (i.e., viability determined by MTS assay), suggesting that nanocurcumin could be more toxic than curcumin *in vitro*[76]. After exposing neuroblastoma cells to nanocurcumin and curcumin for up to 24hrs, they discovered that 6hr and 10hr exposure of

100[μM]$_{eq}$ nanocurcumin led to higher ROS levels (i.e., measured by DCF-DA) compared 100[μM] curcumin. Interestingly, cells that were subjected to 100[μM] curcumin and 100[μM]$_{eq}$ nanocurcumin showed increased expression of caspase 3/7, suggesting that curcumin may have exhibited pro-apoptotic effects[76]. As shown in Table-1, different doses and drug treatment durations are utilized for studies investigating the protective potential of curcumin against H_2O_2. In our cytoprotection studies, curcumin treatment doses ranged between 1-5[μM] for 6hrs or 24hrs against H_2O_2 exposure of 24hrs, which are comparable to other dose ranges and time (Table-1). Curcumin and nanoparticles of curcumin can behave differently *in vitro* and while it is likely that a decrease in ROS levels is directly correlated to cytoprotection it is not a certainty. This could also depend on how curcumin is compartmentalized in the cell (eg. mitochondria, nucleus, lysosome or not, lipid membranes/rafts)[77]. Further studies are required to determine the other players involved in the mechanism of cytoprotection via antioxidation. Differences in the nanoformulation of curcumin and the nature of the nanoparticle can alter the nano-drug response profile *in vitro.* Some evidence suggests that a nano-drug of curcumin is well-tolerated and promotes greater antioxidation capacity (i.e., lowering of ROS, activation of CAT and SOD) compared to curcumin even in malignant cells. However, additional studies are required to investigate curcumin's pro-apoptotic effects *in vitro*[78] and it might be necessary to compare the effects of cell lines like THP-1 to primary human monocyte/macrophages, such as could be isolated directly from blood or bone marrow. Additionally, studies should be extended to direct measures of ROS, or anti-inflammatory effects that are relevant to macrophage biology and their roles pathophysiologically[79].

Others have investigated the cytoprotective potential of nanoparticles of curcumin and curcumin in non-macrophage cells *in vivo and in vitro,* which are relevant to our work as they also were using similar doses or else determining antioxidant (specifically to hydrogen peroxide) or anti-inflammatory effects. In Table-1, the cytoprotective effect of curcumin was seen when human epithelial cells (ECV304) were pre-treated with curcumin (1-5[μM]) followed by H_2O_2 for

2hrs (i.e., viability determined by MTT assay). By adding an inhibitor of HMOX1 protein, tin protoporphyrin 1X (SnPP), they showed that curcumin was no longer protective against H_2O_2, suggesting that the HMOX1 protein was likely mediating the protective effects of curcumin. Another study showed that 14[μM] curcumin was cytoprotective when administered simultaneously with H_2O_2 in HUVECs, despite a concomitant increase in ROS levels. Paradoxically in that study, HUVECs treated with $14[\mu M]_{eq}$ nanocurcumin (encapsulated poly-beta-amino-esters (PBAE) nanogels) did not confer cytoprotection but lowered ROS levels (i.e., cell viability measured using calcein AM red-orange live cell tracer). Primary healthy lung epithelial cells (BEAS-2B) tolerate up to $200[\mu g/mL]_{eq}$ or $544[\mu M]_{eq}$ of nanocurcumin (encapsulated-hollow mesoporous-silica-bovine-serum-albumin; Cur-HMSN-BSA) nanoparticles for 12hr and 24hrs (i.e., determined by MTT assay)[72]. BEAS-2B cells were pre-treated with nanocurcumin (Cur-HMSN-BSA) or curcumin for 12hrs followed by particulate matter ≤2.5μm stress ($PM_{2.5}$, promotes cytotoxicity and inflammatory responses) for 24hrs. They found that nanocurcumin, but not curcumin showed cytoprotection (Table-1). However, both formulations of curcumin decreased ROS levels (measured by DCF-DA assay). These findings further reinforce the uncoupling of colloidal drug trafficking/effects by a nanocarrier from the dose equivalent effect of dissolved drugs, while emphasizing the importance of reference-based comparison when developing nanoformulated API and careful examination *in vitro* prior to *in vivo* study.

Additional findings from *in vivo* studies also demonstrate variable nanopharmacological effects relevant to curcumin. In chicken embryo hearts exposed to AAPH (i.e., ROS generator) immediately followed by curcumin or nanocurcumin (AuNP-C) for 24hrs, those hearts treated with $814[\mu M]_{eq}$ nanocurcumin or the same dose of curcumin promoted a decrease in ROS levels relative to vehicles (empty-nanoparticle controls)[73]. Wang *et. al* investigated the cytoprotective potential of curcumin and nanocurcumin (i.e., curcumin encapsulated polymer) in transendothelial electrical resistance/resistivity (TEER) across blood brain barrier (BBB), in a model of oxidatively stressed MBMECs primary murine endothelial cells[80]. MBMECs that were treated with H_2O_2 for

48hrs showed decreased TEER value, suggesting that H_2O_2 induced breakage of BBB endothelial cells. However, simultaneous administration of 20[μM] curcumin or 20$[\mu M]_{eq}$ nanocurcumin with H_2O_2 for 48hrs protected MBMECs against oxidative stress (i.e., TEER values increased relative to H_2O_2 negative control)[80]. Taken together, these findings may suggest that curcumin or nanoparticles of curcumin can protect primary cells or healthy/non-cancerous cells against oxidative stress, perhaps mediated by decreasing ROS levels.

Uptake, internalization, and biodistribution are important considerations in the development of nanocurcumin as a potential therapeutic. How age, or disease might influence the bioavailability of curcumin or nanocurcumin has not been determined. Many diseases are associated with gut dysbiosis and inflammation. It is interesting to speculate whether studies that used curcumin *in vivo* might have inadvertently been able to elevate the passage of curcumin into the bloodstream due to inflammation[81] but there are no studies to our knowledge that have made a direct comparison in pharmacokinetics/dynamics in healthy, aged, or under-stress conditions comparatively. A comparison of the uptake and internalization between curcumin and nanocurcumin has been done *in vitro*. In one study, flow cytometry data revealed that the mean fluorescent intensity signal for curcumin was higher (+600%) for 10$[\mu M]_{eq}$ nanocurcumin (encapsulated-tannic-acid-poloxamer; Cur-TA-poloxamer) nanoparticles compared to 10[μM] curcumin after 4hrs[82]. Our findings were similar, where we showed that the nanobotanical of curcumin achieved a higher uptake (+91%, 5$[\mu M]_{eq}$) than curcumin at equivalent doses. This might explain the two-fold advantage of HMOX1 induction at equivalent doses by PVDL-005. Variation (~40%) in the proportional measures (uptake fluorescence vs HMOX1 induction) may be due to non-fluorescent/curcumin excipient/API in the nanoformulated botanical. Nanoparticles of curcumin are expected to induce HMOX1 as the main effector of cytoprotection, however, if a cell is generally under stress, HMOX1 is also likely to be induced by that stress, such as elevated ROS. Sarawi *et al.* showed that lung tissues collected from $CuSO_4$-intoxicated rats (i.e., $CuSO_4$ triggers lung injury in rats by causing oxidative stress) treated for 7 days with

80[mg/kg]$_{eq}$ nanocurcumin (liposomal encapsulated curcumin; nCurc) exhibited higher induction of HMOX1 compared to 80[mg/kg] curcumin[83]. This shows that stress plus curcumin can be additive to the induction of HMOX1. In another study, colon tissues collected from ulcerative colitis (UC) mice (i.e., UC was induced using 3% dextran sodium sulfate) that were treated for 6 days with 5[mg/kg]$_{eq}$ nanocurcumin (encapsulated D-mannose-yeast-cell-wall-microparticles; Man-CUR- NYPs) showed higher induction of HMOX1 compared to 5[mg/kg] curcumin[84]. Taken together, nanoparticles of curcumin may be internalized more favourably compared to curcumin *in vitro or in vivo*, allowing for more curcumin to enter the cell and promote greater induction of HMOX1.

4.6 Limitations and future directions

The induction of HMOX1 by curcumin or PVDL-005 could involve additional trans activators than just p-Nrf2 and require further investigation. Moreover, further studies are needed to understand the *in vitro* pharmacokinetics of PVDL-005 and curcumin. An NP-40 whole-cell lysis buffer was used to collect protein lysates from all treated curcumin/PVDL-005 cells as this is standard protocol in the lab. Phosphorylated or p-Nrf2 protein levels were evaluated by western blot. Perhaps isolating both nuclear and cytoplasmic fractions of Nrf2 instead of whole cell lysates could allow for a more accurate assessment of Nrf2 by immunoblotting. Primary mouse cortical cells that were treated with 5[μM] curcumin for 12hrs show an increase in HMOX1 and this induction appears to be dependent on both cytoplasmic and nuclear Nrf2 levels[38]. Recent data suggest that HMOX1 protein itself can behave as a transcriptional co-factor (i.e., independent of its enzymatic activity in the cytoplasm), where it can translocate into the nucleus and mediate the activity of other transcriptional factors or promote tumour progression via inactivation of nuclear factor- κB (NF-κB) [54]. NF-κB, activator protein (AP-1) and Bach1 are other transcriptional factors that can also regulate HMOX1 induction, which may contribute to how curcumin induces HMOX1 expression[85]. NF- κB is normally present in the cytosol, where it is bound to the inhibitory component IκB, which undergoes phosphorylation,

allowing for it to translocate to the nucleus. Hill-Kapturczak *et al.* co-incubated human renal proximal tubule cells (HPTCs) with 8[μM] curcumin with BAY 11-7082 (i.e., an inhibitor of IκB phosphorylation) and found that HMOX1 mRNA and protein levels were abolished (i.e., BAY 11-7082 did not affect HMOX1 protein levels)[86]. This suggests that NF-kB may play a role in the induction of HMOX1 by curcumin. Our study was limited in that we have only explored the canonical Nrf2 mediated mechanism of curcumin induction of HMOX1. All transcription factors induce multiple genes, and so are relevant to be considered in determining biological equivalency. It might be of interest to compare nanocurcumin to curcumin, or dose-dependent changes by RNAseq analysis for an unbiased approach to these studies in future to better understand the paradoxical nature of curcumin effects or lack thereof.

Based on our results, it is unclear whether nanoparticles escape lysosomal degradation. It may be worth investigating if PVDL-005 localizes in the lysosome or can escape lysosomal degradation. Using ER tracker and lysotracker (i.e., to track the lysosome), Yang *et al.* discovered that nanocurcumin (curcumin encapsulated polyethylene glycol-polytrimethylene carbonate (PEG-PTMC) nanoparticles; C6-NPs) were primarily distributed within the ER and the lysosome of MDCK canine kidney epithelial cells, which could impact the bioavailability of curcumin *in vitro* [87]. The microscopy laser confocal scanning microscopy images also showed that nanocurcumin produces granular-like green fluorescent signals. In the same study, they compared the pharmacokinetics of nanocurcumin and curcumin by treating C57BL/6 mice with 5[mg/kg]$_{eq}$/[mg/kg] and collected the plasma. They found that there were higher concentrations of curcumin in nanocurcumin-treated mice compared to curcumin-treated mice, suggesting that nanoparticles of curcumin can enhance the bioavailability of curcumin [87]. Sunoqrot *et al.* showed that 10[μM]$_{eq}$ nanocurcumin (encapsulated-tannic-acid-poloxamer; Cur-TA-poloxamer) had greater bioaccumulation compared to curcumin in MCF-7 and MDA-MB-231 breast cancer cells after 4hrs by confocal microscopy, which also helps to demonstrate that more curcumin enters cells when encapsulated by nanoparticles[82], even in

non-macrophage cells. Further investigation is required to understand where HMOX1 is localized under normal or stressed conditions and how curcumin mediates HMOX1 induction in macrophages. Moreover, future experiments could investigate the drug-release profile of curcumin in PVDL-005, and introduce several more time points (e.g., 15mins-24 hrs) to compare and contrast the kinetics of internalization between 2.5/5[μM]$_{eq}$ PVDL-005 and 2.5/5[μM] curcumin by flow cytometry, and confocal/super-resolution microscopy.

Curcumin or PVDL-005 (nanoparticle of curcumin) may not be cytoprotective in the presence of H_2O_2 (i.e., direct ROS) in macrophages but might be in the context of other stressors (eg, LPS), or other cell types or variable macrophage polarization and could be considered in further studies. Curcumin and its derivatives have been shown to exert anti-inflammatory and anti-oxidative effects in RAW 264.7 macrophages[88]. It may be possible to investigate curcumin's efficacy in the context of acute or chronic inflammation by targeting known inflammatory targets (i.e., NF- κB, iNOS, COX-2, HMOX1) and by measuring cytokine levels (IL-1, IL-12, MCP-1/2, TNF-α and INFγ) from collected conditioned media of macrophages treated with curcumin and PVDL-005. Identifying the macrophage phenotype (M1 or M2) after treatment curcumin or PVDL-005 also warrants further investigation. Differentiated macrophages can take-on a pro-inflammatory M1 or anti-inflammatory M2 phenotype. The presence of curcumin may promote or limit this polarization directly. This physiological phenomenon can be replicated *in vitro* where THP-1 monocytes are differentiated into adherent macrophages using PMA and then polarized to an M1 phenotype using IFN-γ and LPS or to an M2 phenotype with IL-4[20]. Interestingly, 25[μM] curcumin (i.e., a treatment dose 5 times higher than the dose used in our assay) was reported to polarize differentiated macrophages to anti-inflammatory M2 phenotypes[89]. The differential in the treatment doses might be due to potential differences in protein expression profiles between RAW 274.7 murine macrophages and THP-1 human macrophages[90]. Polarization to an anti-inflammatory M2 after curcumin or PVDL-005 treatment may promote macrophage cytoprotection through enhanced anti-inflammatory autocrine and

paracrine release. Treated macrophages could be distinguished from inflammatory M1s by probing for CD80 or to anti-inflammatory M2 (CD163, CD206)[65]. Sun *et al.* subjected mice to particulate matter ≤2.5μm ($PM_{2.5}$) for up to 13 days to induce an inflammatory response in the lung. The next day, mice were treated with curcumin or nanocurcumin (Cur-HMSN-BSA; Curcumin encapsulated hollow mesoporous silica bovine serum albumin nanoparticles) for three days and mice were then sacrificed[72]. Major tissues like the lung were isolated and stained with CD80 and CD206 antibodies. Flow cytometry data showed that nanocurcumin could promote macrophage polarization with less pro-inflammatory M1 and more anti-inflammatory M2 phenotypes. Both curcumin and nanocurcumin lowered the population of M1s[72]. Investigating the cytoprotective potential of curcumin in the context of inflammation would allow for an improved understanding of HMOX1 as a regulator of both inflammation and oxidative stress. The polarization of macrophages by curcumin or PVDL-005 might impact the cytoprotective potential of macrophages by modifying the inflammatory profile of macrophages.

In the future, it may be possible to investigate the effects of other nanoformulations, such as PVDL-002/-003 intracellularly. PVDL-002 and -003 were nanoformulated from turmeric in concert with 3 other botanicals. These two formulations showed greater potent direct antioxidant capacity and thus could be pursued as future formulations for cellular cytoprotection assays. Working with PVDL-002 and -003 would require building a suitable antioxidant reference standard for curcumin including the 3 other APIs. Moreover, determining the percent composition of other polyphenolic compounds in these PVDL turmeric nanoparticles may be advantageous as these botanicals are likely a heterogeneous mixture of curcumin (i.e., the API) and other endogenous compounds. The objective goal of FDA botanical development is to enhance the opportunity for heterogenous API therapeutic development through additive or synergistic properties of the formulation.

NAC is a potent antioxidant that can target oxidant species directly. NAC can exert indirect effects also as it is a precursor of cysteine, a non-essential amino acid that is key for GSH synthesis to promote antioxidation[91]. NAC was selected as a positive control due to evidence of its ability to lower ROS levels relative to an H_2O_2 negative control in THP-1 macrophages (i.e., complete reduction in ROS levels was not achieved)[42]. Alternatively, hemin could be introduced as a positive control as empirical evidence shows that it induces HMOX1 expression.

It may be worth investigating drug cytotoxicity (i.e., curcumin, PVDL-005, H_2O_2) in THP-1 human macrophages using other cell viability/cytotoxicity assays. Our cell viability studies were performed using PrestoBlue cell viability reagent, an assay developed to detect cell viability/cytotoxicity with or without drug/stimulus. PrestoBlue is a resazurin-based compound, where the assay is dependent on the ability of viable and metabolically active cells to reduce resazurin to resorufin (i.e., through NADPH and other mitochondrial enzymes) that can be detected by fluorescence or absorbance[92]. The MTT/MTS assay is the most used viability assay, where tetrazolium is reduced by cytosolic dehydrogenases to formazan. The absorbance of formazan can be correlated to cell viability[93]. PrestoBlue has been shown to be a suitable method to determine cell viability of human endothelial cells to plant extracts as ED_{50} values were comparable to EC_{50} determined by MTT cell viability assay[92]. Incorporating PrestoBlue into assays provides a non-toxic/lethal method to assess viability. For example, PrestoBlue can be relied upon to accurately quantify viable cells within bioartificial tissues and 3D extracellular matrix (ECM) scaffolds. The limitations of the assay are that longer assay incubation times and larger cell numbers can slow the reduction of resazurin to resorufin. Another limitation is that resorufin can further be reduced to hydroresorufin[94]. These limitations could affect the accuracy of the fluorescence reading and the interpretation of cell viability. Curcumin was reported as being tolerated with treatments up to 30[μM] in THP-1 macrophages when viability was measured by MTT assay[95]. An alternative to the PrestoBlue or MTT is the LDH cytotoxicity

assay. Lactate dehydrogenase converts NADH to NAD+ and pyruvate to L-lactate during glycolysis[96]. LDH is released into the extracellular environment in response to cell or drug-induced cytotoxicity. In the assay, LDH (i.e., released by the cell into cell culture media) will oxidize lactate to pyruvate, then reacts with iodonitrotetrazolium chloride (INT) to form formazan, which is inversely correlated to cell viability by absorbance[96]. Chan *et al*. measured human osteoblast response to curcumin by LDH assay and found that these cells could safely be treated with curcumin up to 12.5[μM] curcumin for 12hrs[97]. No studies have incorporated the LDH cytotoxicity assay of curcumin on THP-1 macrophages or combined assays to determine if there are differences and this could be of interest to future experimental designs. Different assays may produce a differential in the cell viability readings. Moreover, future studies may look to investigate whether curcumin can influence glycolysis or anaerobic/aerobic respiration intracellularly. However, proper calibration, defined incubation times and terminology used to define the readout of the assay (i.e., cytotoxicity vs metabolic activity/cell viability) must be considered when working with cell viability assays.

4.7 Conclusions

In conclusion, our study characterizes PVDL-005 (a nanobotanical of curcumin derived from turmeric root) and highlights the importance of QAC and GMP for nanobotanical development. Further, our findings establish that curcumin and PVDL-005 at molar equivalent doses elicit twofold more HMOX1 induction by the nanoformulation, which may be due to greater bioaccumulation of curcumin via PVDL-005 (i.e., relative to curcumin) by THP-1 macrophages. Neither curcumin nor PVLD-005 was cytoprotective against H_2O_2 in THP-1 macrophages. Additional studies are needed to understand what other constituents are involved in the transactivation of HMOX1 by curcumin and/or PVDL-005 to validate HMOX1 as the mechanism of action for cytoprotection (antioxidant or anti-inflammatory) in determining bioequivalence (i.e., dose equivalence between two drug formulations) pharmacologically for an effective therapeutic candidate.

References

1 Kloc M, Ghobrial RM, Wosik J, *et al.* Macrophage functions in wound healing. *J Tissue Eng Regen Med* 2019;**13**:99–109. doi:10.1002/term.2772

2 Krzyszczyk P, Schloss R, Palmer A, *et al.* The Role of Macrophages in Acute and Chronic Wound Healing and Interventions to Promote Pro-wound Healing Phenotypes. *Front Physiol* 2018;**9**:419. doi:10.3389/fphys.2018.00419

3 Stamenkovic I. Extracellular matrix remodelling: the role of matrix metalloproteinases. *J Pathol* 2003;**200**:448–64. doi:10.1002/path.1400

4 Wang C, Ma C, Gong L, *et al.* Macrophage Polarization and Its Role in Liver Disease. *Front Immunol* 2021;**12**:803037. doi:10.3389/fimmu.2021.803037

5 Yap J, Irei J, Lozano-Gerona J, *et al.* Macrophages in cardiac remodelling after myocardial infarction. *Nat Rev Cardiol* 2023;**20**:373–85. doi:10.1038/s41569-022-00823-5

6 Chen GY, Nuñez G. Sterile inflammation: sensing and reacting to damage. *Nat Rev Immunol* 2010;**10**:826–37. doi:10.1038/nri2873

7 Desmoulière A, Geinoz A, Gabbiani F, *et al.* Transforming growth factor-beta 1 induces alpha-smooth muscle actin expression in granulation tissue myofibroblasts and in quiescent and growing cultured fibroblasts. *J Cell Biol* 1993;**122**:103–11. doi:10.1083/jcb.122.1.103

8 Leuschner F, Rauch PJ, Ueno T, *et al.* Rapid monocyte kinetics in acute myocardial infarction are sustained by extramedullary monocytopoiesis. *J Exp Med* 2012;**209**:123–37. doi:10.1084/jem.20111009

9 Holl J, Kowalewski C, Zimek Z, *et al.* Chronic Diabetic Wounds and Their Treatment with Skin Substitutes. *Cells* 2021;**10**. doi:10.3390/cells10030655

10 Barman PK, Urao N, Koh TJ. Diabetes induces myeloid bias in bone marrow progenitors associated with enhanced wound macrophage accumulation and impaired healing. *J Pathol* 2019;**249**:435–46. doi:10.1002/path.5330

11 Mirza R, DiPietro LA, Koh TJ. Selective and specific macrophage ablation is detrimental to wound healing in mice. *Am J Pathol* 2009;**175**:2454–62. doi:10.2353/ajpath.2009.090248

12 Raja SN, Carr DB, Cohen M, *et al.* The revised International Association for the Study of Pain definition of pain: concepts, challenges, and compromises. *Pain* 2020;**161**:1976–82. doi:10.1097/j.pain.0000000000001939

13 Vasconcelos DP, Jabangwe C, Lamghari M, *et al.* The Neuroimmune Interplay in Joint Pain: The Role of Macrophages. *Front Immunol* 2022;**13**:812962. doi:10.3389/fimmu.2022.812962

14 Chen O, Donnelly CR, Ji R-R. Regulation of pain by neuro-immune interactions between macrophages and nociceptor sensory neurons. *Curr Opin Neurobiol* 2020;**62**:17–25. doi:10.1016/j.conb.2019.11.006

15 Garrison SR, Stucky CL. The dynamic TRPA1 channel: a suitable pharmacological pain target? *Curr Pharm Biotechnol* 2011;**12**:1689–97. doi:10.2174/138920111798357302

16 Bozza MT, Jeney V. Pro-inflammatory Actions of Heme and Other Hemoglobin-Derived DAMPs. *Front Immunol* 2020;**11**:1323. doi:10.3389/fimmu.2020.01323

17 Pradhan P, Vijayan V, Gueler F, *et al.* Interplay of Heme with Macrophages in Homeostasis and Inflammation. *Int J Mol Sci* 2020;**21**. doi:10.3390/ijms21030740

18 Naito Y, Takagi T, Higashimura Y. Heme oxygenase-1 and anti-inflammatory M2 macrophages. *Arch Biochem Biophys* 2014;**564**:83–8. doi:10.1016/j.abb.2014.09.005

19 Landis RC, Quimby KR, Greenidge AR. M1/M2 Macrophages in Diabetic Nephropathy: Nrf2/HO-1 as Therapeutic Targets. *Curr Pharm Des* 2018;**24**:2241–9. doi:10.2174/1381612824666180716163845

20 Chanput W, Mes JJ, Wichers HJ. THP-1 cell line: an in vitro cell model for immune modulation approach. *Int Immunopharmacol* 2014;**23**:37–45. doi:10.1016/j.intimp.2014.08.002

21 Liu S, Yang W, Li Y, *et al.* Fetal bovine serum, an important factor affecting the reproducibility of cell experiments. *Sci Rep* 2023;**13**:1942. doi:10.1038/s41598-023-29060-7

22 Kimiz-Gebologlu I, Demirden SF, Oncel SS. A study of the THP-1 cell line as the potential biologics production platform with the emphasis on serum-free media substitution for economic expediency. *Biotechnol J* 2022;**17**:e2200154. doi:10.1002/biot.202200154

23 Marigliani B, Balottin LBL, Augusto E de FP. Adaptation of Mammalian Cells to Chemically Defined Media. *Curr Protoc Toxicol* 2019;**82**:e88. doi:10.1002/cptx.88

24 Kim DS, Park SY, Kim JK. Curcuminoids from Curcuma longa L. (Zingiberaceae) that protect PC12 rat pheochromocytoma and normal human umbilical vein endothelial cells from betaA(1-42) insult. *Neurosci Lett* 2001;**303**:57–61. doi:10.1016/s0304-3940(01)01677-9

25 Akaberi M, Sahebkar A, Emami SA. Turmeric and Curcumin: From Traditional to Modern Medicine. *Adv Exp Med Biol* 2021;**1291**:15–39.

doi:10.1007/978-3-030-56153-6_2

26 Adepu S, Ramakrishna S. Controlled Drug Delivery Systems: Current Status and Future Directions. *Molecules* 2021;**26**. doi:10.3390/molecules26195905

27 Gupta SC, Patchva S, Aggarwal BB. Therapeutic roles of curcumin: lessons learned from clinical trials. *AAPS J* 2013;**15**:195–218. doi:10.1208/s12248-012-9432-8

28 Nelson KM, Dahlin JL, Bisson J, *et al.* The Essential Medicinal Chemistry of Curcumin. *J Med Chem* 2017;**60**:1620–37. doi:10.1021/acs.jmedchem.6b00975

29 Ventola CL. Progress in Nanomedicine: Approved and Investigational Nanodrugs. *P T* 2017;**42**:742–55.

30 Moghimi SM, Hunter AC, Murray JC. Long-circulating and target-specific nanoparticles: theory to practice. *Pharmacol Rev* 2001;**53**:283–318.

31 Mitchell MJ, Billingsley MM, Haley RM, *et al.* Engineering precision nanoparticles for drug delivery. *Nat Rev Drug Discov* 2021;**20**:101–24. doi:10.1038/s41573-020-0090-8

32 Mohammad O, Faisal SM, Ahmad N, *et al.* Bio-mediated synthesis of 5-FU based nanoparticles employing orange fruit juice: a novel drug delivery system to treat skin fibrosarcoma in model animals. *Sci Rep* 2019;**9**:12288. doi:10.1038/s41598-019-48180-7

33 Gao C, Zhou Y, Chen Z, *et al.* Turmeric-derived nanovesicles as novel nanobiologics for targeted therapy of ulcerative colitis. *Theranostics* 2022;**12**:5596–614. doi:10.7150/thno.73650

34 Chopra H, Dey PS, Das D, *et al.* Curcumin Nanoparticles as Promising Therapeutic Agents for Drug Targets. *Molecules* 2021;**26**. doi:10.3390/molecules26164998

35 Rostamzadeh F, Jafarinejad-Farsangi S, Ansari-Asl Z, *et al.* Treatment for Myocardial Infarction: In Vivo Evaluation of Curcumin-Loaded PEGylated-GQD Nanoparticles. *J Cardiovasc Pharmacol* 2023;**81**:361–72. doi:10.1097/FJC.0000000000001410

36 Banerjee A, Kunwar A, Mishra B, *et al.* Concentration dependent antioxidant/pro-oxidant activity of curcumin studies from AAPH induced hemolysis of RBCs. *Chem Biol Interact* 2008;**174**:134–9. doi:10.1016/j.cbi.2008.05.009

37 Cheppudira B, Fowler M, McGhee L, *et al.* Curcumin: a novel therapeutic for burn pain and wound healing. *Expert Opin Investig Drugs* 2013;**22**:1295–303. doi:10.1517/13543784.2013.825249

38 Park J-Y, Sohn H-Y, Koh YH, *et al.* Curcumin activates Nrf2 through PKCδ-

mediated p62 phosphorylation at Ser351. *Sci Rep* 2021;**11**:8430. doi:10.1038/s41598-021-87225-8

39 Gupta P, Jordan CT, Mitov MI, *et al.* Controlled curcumin release via conjugation into PBAE nanogels enhances mitochondrial protection against oxidative stress. *Int J Pharm* 2016;**511**:1012–21. doi:10.1016/j.ijpharm.2016.07.071

40 Jeong GS, Oh GS, Pae H-O, *et al.* Comparative effects of curcuminoids on endothelial heme oxygenase-1 expression: ortho-methoxy groups are essential to enhance heme oxygenase activity and protection. *Exp Mol Med* 2006;**38**:393–400. doi:10.1038/emm.2006.46

41 Giambelluca S, Ochs M, Lopez-Rodriguez E. Resting time after phorbol 12-myristate 13-acetate in THP-1 derived macrophages provides a non-biased model for the study of NLRP3 inflammasome. *Front Immunol* 2022;**13**:958098. doi:10.3389/fimmu.2022.958098

42 Palacio JR, Markert UR, Martínez P. Anti-inflammatory properties of N-acetylcysteine on lipopolysaccharide-activated macrophages. *Inflamm Res* 2011;**60**:695–704. doi:10.1007/s00011-011-0323-8

43 Estany S, Palacio JR, Barnadas R, *et al.* Antioxidant activity of N-acetylcysteine, flavonoids and alpha-tocopherol on endometrial cells in culture. *J Reprod Immunol* 2007;**75**:1–10. doi:10.1016/j.jri.2007.01.007

44 Aiyer A, Das T, Whiteley GS, *et al.* The Efficacy of an N-Acetylcysteine-Antibiotic Combination Therapy on Achromobacter xylosoxidans in a Cystic Fibrosis Sputum/Lung Cell Model. *Biomedicines* 2022;**10**. doi:10.3390/biomedicines10112886

45 Bhattacharjee S. DLS and zeta potential - What they are and what they are not? *J Control Release* 2016;**235**:337–51. doi:10.1016/j.jconrel.2016.06.017

46 Behzadi S, Serpooshan V, Tao W, *et al.* Cellular uptake of nanoparticles: journey inside the cell. *Chem Soc Rev* 2017;**46**:4218–44. doi:10.1039/c6cs00636a

47 Ke D, Wang X, Yang Q, *et al.* Spectrometric study on the interaction of dodecyltrimethylammonium bromide with curcumin. *Langmuir* 2011;**27**:14112–7. doi:10.1021/la203592j

48 Krishnamoorthy A, Tavoosi N, Chan GKL, *et al.* Effect of curcumin on amyloid-like aggregates generated from methionine-oxidized apolipoprotein A-I. *FEBS Open Bio* 2018;**8**:302–10. doi:10.1002/2211-5463.12372

49 Trovó AG, Nogueira RFP, Agüera A, *et al.* Degradation of sulfamethoxazole in water by solar photo-Fenton. Chemical and toxicological evaluation. *Water Res* 2009;**43**:3922–31. doi:10.1016/j.watres.2009.04.006

50 Michiels R, Gensch N, Erhard B, *et al.* Pulling, failing, and adaptive mechanotransduction of macrophage filopodia. *Biophys J* 2022;**121**:3224–41. doi:10.1016/j.bpj.2022.07.028

51 Rauch C, Feifel E, Amann E-M, *et al.* Alternatives to the use of fetal bovine serum: human platelet lysates as a serum substitute in cell culture media. *ALTEX* 2011;**28**:305–16. doi:10.14573/altex.2011.4.305

52 Park SY, Park DJ, Kim YH, *et al.* Schisandra chinensis α-iso-cubebenol induces heme oxygenase-1 expression through PI3K/Akt and Nrf2 signaling and has anti-inflammatory activity in Porphyromonas gingivalis lipopolysaccharide-stimulated macrophages. *Int Immunopharmacol* 2011;**11**:1907–15. doi:10.1016/j.intimp.2011.07.023

53 Yuan S, Li H, Yang C, *et al.* DHA attenuates Aβ-induced necroptosis through the RIPK1/RIPK3 signaling pathway in THP-1 monocytes. *Biomed Pharmacother* 2020;**126**:110102. doi:10.1016/j.biopha.2020.110102

54 Zhang Y, Lian F, Zhu Y, *et al.* Cyanidin-3-O-beta-glucoside inhibits LPS-induced expression of inflammatory mediators through decreasing IkappaBalpha phosphorylation in THP-1 cells. *Inflamm Res* 2010;**59**:723–30. doi:10.1007/s00011-010-0183-7

55 Lin P-C, Lin S, Wang PC, *et al.* Techniques for physicochemical characterization of nanomaterials. *Biotechnol Adv* 2014;**32**:711–26. doi:10.1016/j.biotechadv.2013.11.006

56 Madkhali OA, Moni SS, Sultan MH, *et al.* Design and characterization of Lactotransferrin peptide-loaded dextran-docosahexaenoic acid nanoparticles: an immune modulator for hepatic damage. *Sci Rep* 2023;**13**:13537. doi:10.1038/s41598-023-40674-9

57 Péret-Almeida L, Cherubino APF, Alves RJ, *et al.* Separation and determination of the physico-chemical characteristics of curcumin, demethoxycurcumin and bisdemethoxycurcumin. *Food Res Int* 2005;**38**:1039–44. doi:10.1016/j.foodres.2005.02.021

58 Yona S, Gordon S. From the Reticuloendothelial to Mononuclear Phagocyte System - The Unaccounted Years. *Front Immunol* 2015;**6**:328. doi:10.3389/fimmu.2015.00328

59 Lunov O, Syrovets T, Loos C, *et al.* Differential uptake of functionalized polystyrene nanoparticles by human macrophages and a monocytic cell line. *ACS Nano* 2011;**5**:1657–69. doi:10.1021/nn2000756

60 Starr T, Bauler TJ, Malik-Kale P, *et al.* The phorbol 12-myristate-13-acetate differentiation protocol is critical to the interaction of THP-1 macrophages with Salmonella Typhimurium. *PLoS One* 2018;**13**:e0193601. doi:10.1371/journal.pone.0193601

61 Pham T-H, Kim M-S, Le M-Q, *et al.* Fargesin exerts anti-inflammatory

effects in THP-1 monocytes by suppressing PKC-dependent AP-1 and NF-κB signaling. *Phytomedicine* 2017;**24**:96–103. doi:10.1016/j.phymed.2016.11.014

62 Song Y, Zhou T, Zong Y, *et al.* Arsenic inhibited cholesterol efflux of THP-1 macrophages via ROS-mediated ABCA1 hypermethylation. *Toxicology* 2019;**424**:152225. doi:10.1016/j.tox.2019.05.012

63 Safar R, Doumandji Z, Saidou T, *et al.* Cytotoxicity and global transcriptional responses induced by zinc oxide nanoparticles NM 110 in PMA-differentiated THP-1 cells. *Toxicol Lett* 2019;**308**:65–73. doi:10.1016/j.toxlet.2018.11.003

64 Cirmi S, Maugeri A, Russo C, *et al.* Oleacein Attenuates Lipopolysaccharide-Induced Inflammation in THP-1-Derived Macrophages by the Inhibition of TLR4/MyD88/NF-κB Pathway. *Int J Mol Sci* 2022;**23**. doi:10.3390/ijms23031206

65 Kologrivova I, Shtatolkina M, Suslova T, *et al.* Cells of the Immune System in Cardiac Remodeling: Main Players in Resolution of Inflammation and Repair After Myocardial Infarction. *Front Immunol* 2021;**12**:664457. doi:10.3389/fimmu.2021.664457

66 Tang F, Xie Y, Cao H, *et al.* Fetal bovine serum influences the stability and bioactivity of resveratrol analogues: A polyphenol-protein interaction approach. *Food Chem* 2017;**219**:321–8. doi:10.1016/j.foodchem.2016.09.154

67 Li P-C, Chen S-C, Hsueh Y-J, *et al.* Gelatin scaffold with multifunctional curcumin-loaded lipid-PLGA hybrid microparticles for regenerating corneal endothelium. *Mater Sci Eng C Mater Biol Appl* 2021;**120**:111753. doi:10.1016/j.msec.2020.111753

68 Lin X, Bai D, Wei Z, *et al.* Curcumin attenuates oxidative stress in RAW264.7 cells by increasing the activity of antioxidant enzymes and activating the Nrf2-Keap1 pathway. *PLoS One* 2019;**14**:e0216711. doi:10.1371/journal.pone.0216711

69 Li H, van Berlo D, Shi T, *et al.* Curcumin protects against cytotoxic and inflammatory effects of quartz particles but causes oxidative DNA damage in a rat lung epithelial cell line. *Toxicol Appl Pharmacol* 2008;**227**:115–24. doi:10.1016/j.taap.2007.10.002

70 Zhang B, Swamy S, Balijepalli S, *et al.* Direct pulmonary delivery of solubilized curcumin reduces severity of lethal pneumonia. *FASEB J* 2019;**33**:13294–309. doi:10.1096/fj.201901047RR

71 Chen X, Zhong Z, Xu Z, *et al.* No protective effect of curcumin on hydrogen peroxide-induced cytotoxicity in HepG2 cells. *Pharmacol Rep* 2011;**63**:724–32. doi:10.1016/s1734-1140(11)70584-9

72 Sun G, Wu X, Zhu H, *et al.* Reactive Oxygen Species-Triggered Curcumin Release from Hollow Mesoporous Silica Nanoparticles for PM2.5-Induced Acute Lung Injury Treatment. *ACS Appl Mater Interfaces* 2023;**15**:33504–13. doi:10.1021/acsami.3c07361

73 Benatti Justino A, Prado Bittar V, Luiza Borges A, *et al.* Curcumin-functionalized gold nanoparticles attenuate AAPH-induced acute cardiotoxicity via reduction of lipid peroxidation and modulation of antioxidant parameters in a chicken embryo model. *Int J Pharm* 2023;**646**:123486. doi:10.1016/j.ijpharm.2023.123486

74 Doggui S, Sahni JK, Arseneault M, *et al.* Neuronal uptake and neuroprotective effect of curcumin-loaded PLGA nanoparticles on the human SK-N-SH cell line. *J Alzheimers Dis* 2012;**30**:377–92. doi:10.3233/JAD-2012-112141

75 Ghoreyshi N, Ghahremanloo A, Javid H, *et al.* Effect of folic acid-linked chitosan-coated PLGA-based curcumin nanoparticles on the redox system of glioblastoma cancer cells. *Phytochem Anal* 2023;**34**:950–8. doi:10.1002/pca.3263

76 Kalashnikova I, Mazar J, Neal CJ, *et al.* Nanoparticle delivery of curcumin induces cellular hypoxia and ROS-mediated apoptosis via modulation of Bcl-2/Bax in human neuroblastoma. *Nanoscale* 2017;**9**:10375–87. doi:10.1039/c7nr02770b

77 Ben-Zichri S, Kolusheva S, Danilenko M, *et al.* Cardiolipin mediates curcumin interactions with mitochondrial membranes. *Biochim Biophys acta Biomembr* 2019;**1861**:75–82. doi:10.1016/j.bbamem.2018.10.016

78 Zhu L, Han MB, Gao Y, *et al.* Curcumin triggers apoptosis via upregulation of Bax/Bcl-2 ratio and caspase activation in SW872 human adipocytes. *Mol Med Rep* 2015;**12**:1151–6. doi:10.3892/mmr.2015.3450

79 Menon VP, Sudheer AR. Antioxidant and anti-inflammatory properties of curcumin. *Adv Exp Med Biol* 2007;**595**:105–25. doi:10.1007/978-0-387-46401-5_3

80 Wang Y, Luo J, Li S-Y. Nano-Curcumin Simultaneously Protects the Blood-Brain Barrier and Reduces M1 Microglial Activation During Cerebral Ischemia-Reperfusion Injury. *ACS Appl Mater Interfaces* 2019;**11**:3763–70. doi:10.1021/acsami.8b20594

81 Kawanishi N, Kato K, Takahashi M, *et al.* Curcumin attenuates oxidative stress following downhill running-induced muscle damage. *Biochem Biophys Res Commun* 2013;**441**:573–8. doi:10.1016/j.bbrc.2013.10.119

82 Sunoqrot S, Orainee B, Alqudah DA, *et al.* Curcumin-tannic acid-poloxamer nanoassemblies enhance curcumin's uptake and bioactivity against cancer cells in vitro. *Int J Pharm* 2021;**610**:121255. doi:10.1016/j.ijpharm.2021.121255

83 Sarawi WS, Alhusaini AM, Alghibiwi HK, *et al.* Roles of Nrf2/HO-1 and ICAM-1 in the Protective Effect of Nano-Curcumin against Copper-Induced Lung Injury. *Int J Mol Sci* 2023;**24**. doi:10.3390/ijms241813975

84 Han X, Luo R, Qi S, *et al.* 'Dual sensitive supramolecular curcumin nanoparticles' in 'advanced yeast particles' mediate macrophage reprogramming, ROS scavenging and inflammation resolution for ulcerative colitis treatment. *J Nanobiotechnology* 2023;**21**:321. doi:10.1186/s12951-023-01976-2

85 Alam J, Cook JL. How many transcription factors does it take to turn on the heme oxygenase-1 gene? *Am J Respir Cell Mol Biol* 2007;**36**:166–74. doi:10.1165/rcmb.2006-0340TR

86 Hill-Kapturczak N, Thamilselvan V, Liu F, *et al.* Mechanism of heme oxygenase-1 gene induction by curcumin in human renal proximal tubule cells. *Am J Physiol Renal Physiol* 2001;**281**:F851-9. doi:10.1152/ajprenal.2001.281.5.F851

87 Yang C, Han M, Li R, *et al.* Curcumin Nanoparticles Inhibiting Ferroptosis for the Enhanced Treatment of Intracerebral Hemorrhage. *Int J Nanomedicine* 2021;**16**:8049–65. doi:10.2147/IJN.S334965

88 Xie Q-F, Cheng J-J, Chen J-F, *et al.* Comparation of Anti-Inflammatory and Antioxidantactivities of Curcumin, Tetrahydrocurcuminand Octahydrocurcuminin LPS-Stimulated RAW264.7 Macrophages. *Evid Based Complement Alternat Med* 2020;**2020**:8856135. doi:10.1155/2020/8856135

89 Gao S, Zhou J, Liu N, *et al.* Curcumin induces M2 macrophage polarization by secretion IL-4 and/or IL-13. *J Mol Cell Cardiol* 2015;**85**:131–9. doi:10.1016/j.yjmcc.2015.04.025

90 Li P, Hao Z, Wu J, *et al.* Comparative Proteomic Analysis of Polarized Human THP-1 and Mouse RAW264.7 Macrophages. *Front Immunol* 2021;**12**:700009. doi:10.3389/fimmu.2021.700009

91 Aldini G, Altomare A, Baron G, *et al.* N-Acetylcysteine as an antioxidant and disulphide breaking agent: the reasons why. *Free Radic Res* 2018;**52**:751–62. doi:10.1080/10715762.2018.1468564

92 Boncler M, Różalski M, Krajewska U, *et al.* Comparison of PrestoBlue and MTT assays of cellular viability in the assessment of anti-proliferative effects of plant extracts on human endothelial cells. *J Pharmacol Toxicol Methods* 2014;**69**:9–16. doi:10.1016/j.vascn.2013.09.003

93 Pascua-Maestro R, Corraliza-Gomez M, Diez-Hermano S, *et al.* The MTT-formazan assay: Complementary technical approaches and in vivo validation in Drosophila larvae. *Acta Histochem* 2018;**120**:179–86. doi:10.1016/j.acthis.2018.01.006

94 Uzarski JS, DiVito MD, Wertheim JA, *et al.* Essential design considerations for the resazurin reduction assay to noninvasively quantify cell expansion within perfused extracellular matrix scaffolds. *Biomaterials* 2017;**129**:163–75. doi:10.1016/j.biomaterials.2017.02.015

95 Soltani B, Ghaemi N, Sadeghizadeh M, *et al.* Curcumin confers protection to irradiated THP-1 cells while its nanoformulation sensitizes these cells via apoptosis induction. *Cell Biol Toxicol* 2016;**32**:543–61. doi:10.1007/s10565-016-9354-9

96 Kaja S, Payne AJ, Naumchuk Y, *et al.* Quantification of Lactate Dehydrogenase for Cell Viability Testing Using Cell Lines and Primary Cultured Astrocytes. *Curr Protoc Toxicol* 2017;**72**:2.26.1-2.26.10. doi:10.1002/cptx.21

97 Chan W-H, Wu H-Y, Chang WH. Dosage effects of curcumin on cell death types in a human osteoblast cell line. *Food Chem Toxicol* 2006;**44**:1362–71. doi:10.1016/j.fct.2006.03.001